IAEA
International Atomic Energy Agency

INDC(NDS)-0541
Distr. AI+MN+NM

INDC International Nuclear Data Committee

Summary Report

Consultants' Meeting on

Prompt Fission Neutron Spectra of Major Actinides

IAEA Headquarters
Vienna, Austria

24-27 November 2008

Prepared by

R. Capote Noy, IAEA Nuclear Data Section, Austria
V. Maslov, Joint Institute for Power and Nuclear Research – Sosny, Belarus
E. Bauge, Commissariat à l'énergie atomique, France
T. Ohsawa, Kinki University, Japan
A. Vorobyev, Petersburg Nuclear Physics Institute, Russia
M.B. Chadwick, Los Alamos National Laboratory, USA
S. Oberstedt, Institute for Reference Materials and Measurements, Belgium

January 2009

Selected INDC documents may be downloaded in electronic form from http://www-nds.iaea.org/indc_sel.html or sent as an e-mail attachment. Requests for hardcopy or e-mail transmittal should be directed to services@iaeand.iaea.org or to:

Nuclear Data Section
International Atomic Energy Agency
PO Box 100
Wagramer Strasse 5
A-1400 Vienna
Austria

Produced by the IAEA in Austria
January 2009

INDC(NDS)-0541
Distr. AI+MN+NM

Summary Report

Consultants' Meeting on

Prompt Fission Neutron Spectra of Major Actinides

IAEA Headquarters
Vienna, Austria

24-27 November 2008

Prepared by

R. Capote Noy, IAEA Nuclear Data Section, Austria
V. Maslov, Joint Institute for Power and Nuclear Research – Sosny, Belarus
E. Bauge, Commissariat à l'énergie atomique, France
T. Ohsawa, Kinki University, Japan
A. Vorobyev, Petersburg Nuclear Physics Institute, Russia
M.B. Chadwick, Los Alamos National Laboratory, USA
S. Oberstedt, Institute for Reference Materials and Measurements, Belgium

Abstract

A Consultants' Meeting on "Prompt Fission Neutron Spectra of Major Actinides" was held at IAEA Headquarters, Vienna, Austria, to discuss the adequacy and quality of the recommended prompt fission neutron spectra to be found in existing nuclear data applications libraries. These prompt fission neutron spectra were judged to be inadequate, and this problem has proved difficult to resolve by means of theoretical modelling. Major adjustments may be required to ensure the validity of such important data. There is a strong requirement for an international effort to explore and resolve these difficulties and recommend prompt fission neutron spectra and uncertainty covariance matrices for the actinides over the neutron energy range from thermal to 20 MeV. Participants also stressed that there would be a strong need for validation of the resulting data against integral critical assembly and dosimetry data.

January 2009

TABLE OF CONTENTS

1. BACKGROUND AND MOTIVATION 7
2. PRESENT STATUS OF EVALUATED DATABASES AND MEASUREMENTS 7
   2.1. n + ^{235}U thermal (important in thermal reactor systems) 7
   2.2. 0.5 MeV n + ^{235}U (important in fast reactor systems) 8
   2.3. n + ^{239}Pu thermal 8
   2.4. 1.5 MeV n + ^{239}Pu (important in fast reactor systems) 9
   2.5. n + ^{245}Cm thermal 9
   2.6. Emissive fission domain 10
3. RECOMMENDED SCOPE 10
   3.1. Nuclides and energy range 10
   3.2. Covariances 10
   3.3. Theory and model development 11
   3.4. Experiments 11
   3.5. Validation 12
4. CONCLUSIONS 12

ANNEXES

A: Agenda 21
B: List of Participants 23
C: Multimodal Madland-Nix Model: Stick to physics or go *ad hoc* fitting?, *T. Ohsawa* 25
D: Actinide prompt fission neutron spectra, *V.M. Maslov* 31
E: Evaluation of precise fission neutron spectra for actinides, *M.B. Chadwick* 37
F: NIIAR measurements of fission neutron spectra: Summary based on Russian publications and EXFOR database, *V. Pronyaev* 39
G: Ratio of prompt fission neutron spectra from ^{252}Cf(sf) and ^{235}U(n_{th},f) reactions, *V. Pronyaev* 51
H: Recent measurements of the prompt neutron emission spectrum from neutron-induced fission of ^{235}U, *N.V. Kornilov, et al.* 53
I: Measurements of angular and energy distributions of prompt neutrons from thermal neutron-induced fission of ^{235}U(n_{th},f), *A.S. Vorobyev, et al.* 63
J: A note on the effect of angular anisotropy of neutron emission in the fragment center-of-mass system, *T. Ohsawa* 71

1. Background and Motivation

The energy spectrum of prompt neutrons emitted in fission plays an important role in many applications in nuclear science. In particular, accurate predictions of nuclear criticality using neutron transport codes are dependent on the underlying nuclear data, especially the fission spectrum. The high sensitivity of calculated quantities to fission data has been recently emphasized by researchers in many groups around the world that are working on conventional as well as advanced reactors, and non-proliferation applications.

While the accuracy of fission cross-section and neutron multiplicities (nubar) in the relevant energy range have been steadily improved, we are faced with the situation that existing measured prompt fission neutron spectra (PFNS) are in many cases discrepant, and that different PFNS theoretical models give differing predictions. Furthermore, the reactor community has provided feedback on the fission spectra that they perceive as 'working well' within their reactor simulations and integral experiments, though this feedback is sometimes contradictory compared to differential fission cross-section and PFNS experimental data and theories. There are some biases in k_{eff} (up to 300 pcm) in MOX fuel benchmarks, while in other cases similar biases appear to be removed by "tweaking" the evaluated data files. We are now in the situation that the PFNS evaluated databases used in nuclear science applications, from the USA (ENDF/B-VII [1]), Europe (JEFF3.1 [2]), Japan (JENDL3.3 [3]) and Russia (RUSFOND [4]) are essentially rather similar, at least for ^{235}U and ^{239}Pu, yet a number of old (1985-1989) and new measurements, and the works of Maslov *et al.* and Kornilov *et al.* [5-7], point to major changes that may be needed. A new major evaluated actinide file JENDL/AC-2008 has been recently released [8] where new PFNS evaluations of ^{232}Th, ^{237}Np and ^{241}Am were included.

We believe there is a need for internationally coordinated efforts to determine the prompt fission neutron spectra for actinides in ENDF format – especially the major actinides ^{235,238}U and ^{239}Pu up to 20 MeV. The outcome would be a recommended evaluation of prompt fission spectra with covariances from thermal to 20 MeV for the major actinides, including validation against integral critical assembly (k_{eff}) and dosimetry data. Such studies and the resulting recommended database could be best accomplished by means of an IAEA Coordinated Research Project (CRP).

2. Present Status of Evaluated Databases and Measurements

2.1. n + ^{235}U thermal (important in thermal reactor systems) - Figs.1 and 2

Both ENDF/B-VII and JEFF3.1 adopted ENDF/B-VI thermal data, and the fission spectrum of JENDL-3.3 is also very similar to ENDF/B-VI evaluation. The latest RUSFOND file uses ENDF/B-VII. These databases implemented either the Madland-Nix model [9], or in the case of JENDL3.3, a refined version of Madland-Nix model [10, 11]. The PFNS shape of these Madland-Nix model calculations appears to have been fitted to the 0.5-MeV Johansson data [12] and "extrapolated" to the thermal point. On the other hand, the 2008 evaluation by Maslov *et al.* [13] follows the Kornilov *et al.* method [5], and has a significantly higher spectrum below 1 MeV (e.g. 15% higher at 0.1 MeV and below), and a softer spectrum at higher emission energies (e.g. lower by 8% above 10 MeV). The different low-energy behaviour in the Maslov/Kornilov evaluation is attributed to the emphasis on a particular set of experimental data for thermal neutron-induced fission as constraints for model parameter adjustments. However, equally good fits were obtained in the latter approach of the measured data sets, except those of Johansson *et al.* (1975) at 0.5 MeV [12] and Boykov *et al.* (1991) at 2.9 MeV [14].

The experimental data were summarized by WPEC Subgroup 9, which noted some contradictions amongst the various measurements [15]. The measurements by Starostov *et al.* [16] extends down to 50 keV (and are the basis for the Kornilov/Maslov evaluation at the lower energies); Wang Yufeng *et al.* [17] also extended down to 50 keV (but their lowest measured points appear incorrect); and Lajtai *et al.* [18] reported data down to 30 keV, and at low energies below 1 MeV the measured values are consistent with the higher values measured by Starostov *et al.* [16]. The low-energy behaviour (below 1 MeV emission energy) defined by Starostov *et al.* [16] is confirmed by new data presented at this meeting by Vorobyev *et al*[1]. New JRC IRMM data [19] also agree with Starostov *et al.* [16] at outgoing energy range of 0.8-8 MeV. In the high emission energy region, integral data testing by Mannhart (see below for reference and further comments), using threshold dosimetry reactions, appears to point to a fission spectrum that is harder than measured in these Laboratory experiments (and the ENDF/JEFF/JENDL evaluations tend to agree better with these Mannhart data than does the Maslov/Kornilov [13] evaluation). Recently-measured preliminary data by the JRC IRMM group (Hambsch *et al.*) at Budapest suggest a harder spectrum (e.g. than Starostov *et al.* [16] and Wang *et al.* [17]) at higher energies, and are in reasonable agreement with ENDF/JEFF/JENDL – but at present they do not extend below 0.8 MeV outgoing energy (future detector upgrades may allow measurements to be made down to 100 keV). Finally we note once again that the spectra shapes measured at higher energies by Johansson *et al.* [12] (0.5 MeV) and Boykov *et al.* [14] (2.9 MeV) impact results in a model calculation at thermal energy, resulting in possible additional inconsistencies.

2.2. 0.5 MeV n + ^{235}U (important in fast reactor systems) - Fig.3

At 0.5 MeV (or 1 MeV), the evaluations in ENDF/B-VII, JEFF3.1 (ENDF/B-VI), and JENDL3.3 are very similar. The latest RUSFOND file uses ENDF/B-VII. And again, the Maslov/Kornilov [13] evaluation is significantly higher at low energies (about 20% higher at 0.1 MeV) and significantly softer at high energies (about 8% lower at 10 MeV). Similarly to the thermal energies, the low-energy behaviour in the Maslov/Kornilov [13] evaluation could be partly attributed to a different weighting of the experimental data sets adopted to constrain the model parameter adjustments.

Measurements exist by Johansson *et al.* [12], Trufanov *et al.* [20], Staples *et al.* [21], and new Geel data [19]. The data of Johansson *et al.* [12] differ somewhat to the other data sets, with the ENDF/B-VII, JEFF, and JENDL agreeing better with these data as opposed to the other sets. Preliminary LANL dosimetry data testing [22], based on ^{169}Tm(n,2n) and ^{191}Ir(n,2n) activation measurements in Godiva suggest that the ENDF/B-VII high-energy spectrum (> 8 MeV) should be softened. The Geel data [19] need more work to understand the measured angular variations, although these data also indicate a softer spectrum at higher neutron energies than is given in ENDF/B-VII.

2.3. n + ^{239}Pu thermal - Fig.4

As was the case for ^{235}U, the ENDF/B-VII, JENDL3.3 and JEFF3.1 evaluations are very similar, but the Kornilov/Maslov evaluation is higher at lower emission energies below 1 MeV (e.g. 15% higher at 0.1 MeV), and the Kornilov/Maslov evaluation is lower in the 2-8 MeV outgoing energy region. The latest RUSFOND file uses JEFF3.1.

[1] Neutron efficiency was obtained from Monte-Carlo calculations of the experimental setup and detectors, and has not been measured using Cf sources. Efficiency measurements are planned.

There are four experimental measurements, though three come from the same group at Scientific-Research Institute of Atomic Reactors, Dimitrovgrad, Russia (NIIAR): Starostov *et al.* (1983) [16], Nefedov *et al.* (1983) [23], and Bojtsov *et al.* (1983) [24]. A recent review has been undertaken by Pronyaev (Annex F) on PFNS measurements carried out at NIIAR, where detailed information on the experimental setup is made available. The fourth measurement is by Lajtai *et al.* (1985) [18]. Below 0.1 MeV emission energy, three of these data sets appear to be consistent (and are well represented by the Kornilov/Maslov evaluation), and are higher than the Lajtai measurement. Over the higher emission energy region (2-8 MeV), the data of Nefedov and Starostov are well represented by ENDF/B-VII, JENDL3.3 and JEFF3.1, whereas the Kornilov/Maslov evaluation under predicts these data.

2.4. 1.5 MeV n + ^{239}Pu (important in fast reactor systems)

As was the case for ^{235}U, the ENDF/B-VII, JENDL3.3 and JEFF evaluations are very similar, but the Kornilov/Maslov [25] evaluation is higher at the lower emission energy below 1 MeV (e.g. 15% higher at 0.1 MeV), and Kornilov/Maslov [25] evaluation is lower in the 2-8 MeV outgoing energy region. The latest RUSFOND file uses JEFF3.1.

There are measurements at 1.5 MeV by Staples *et al.* [21] (above ~1.5 MeV outgoing energy, extending up to almost 15 MeV). There are also measurements by Sukhikh *et al.* [26] from 2 to 13 MeV outgoing energy. The Kornilov/Maslov evaluation exhibits better agreement with the Sukhih *et al.* [26] data, whereas ENDF/B-VII appears to agree better with Staples *et al.* [21] data. Over the 8-13 MeV region, both Staples *et al.* [21] and Sukhih *et al.* [26] data appear to be lower than ENDF/B-VII. Additionally, preliminary tests of LANL dosimetry data [22] using ^{169}Tm(n,2n) and ^{191}Ir(n,2n) activation experiments in Jezebel suggest that the ENDF/B-VII high-energy spectrum (> 8 MeV) should be softened.

2.5. n + ^{245}Cm thermal - Fig.5

Due to large thermal fission cross sections (2020 b) and a long half-life (8532 y), ^{245}Cm represents a typical example of an important minor actinide. The PFNS of thermal-induced fission on ^{245}Cm was measured from 100 keV up to 10.5 MeV by Drapchinsky *et al.* (1999) [27]. Figure 5 shows the calculated and experimental data relative to the Maxwellian distribution with T_M = 1.385 MeV. The following calculations/evaluations are included:

- Kornilov/Maslov 2008 - calculated by Maslov on the basis of systematics by Kornilov [5];
- Full acceleration - calculated by Ohsawa using the multimodal Madland-Nix model, on the assumption that all neutrons are emitted from fully accelerated fission fragments (corresponds to the JENDL/AC-2008 library evaluation [8]);
- TF60-NEDA40 – calculated by Ohsawa using the multimodal Madland-Nix model, but on the assumption that some fraction of the neutrons was emitted during acceleration (NEDA). 40% of the neutrons are assumed to be emitted from fission fragments at 60% acceleration of the final kinetic energy in the *standard-2 mode* fission. No NEDA was assumed for other fission modes, because of the lower available excitation energy. Mode branching ratios and average fragment masses were calculated with the Wang-Hu model [28]; level density parameters were adopted from the Generalized Superfluid Model as proposed by Ignatyuk [29];
- JENDL-3.3: evaluation by Maslov *et al.* [30], using the single-modal Madland-Nix model [9].

As was the case for ^{235}U, the JENDL3.3 (adopted also for the ENDF/B-VII and JEFF3.1 libraries) and the JENDL/AC-2008 evaluations are very similar, but the Kornilov/Maslov evaluation is higher at the lower emission energy below 1 MeV. Similar behavior was

obtained when the newer JENDL/AC-2008 calculation was performed, which corresponds to the *Full-acceleration* case derived by Ohsawa. On the other hand, for the low-energy region of emitted neutrons less than 3 MeV, no substantial difference can be seen between the evaluations of Kornilov/Maslov and TF60-NEDA40 calculations; while in the higher energy region, Kornilov/Maslov evaluation tends to be much higher than the TF60-NEDA calculations. The latter effect might be an indication for a new analysis of fission energy release and kinetic energies of the ^{245}Cm fission fragments in the systematics by Kornilov *et al.* [5]. Compared with measurements, the full-acceleration calculation tends to give higher values in the MeV-region and lower values below 1 MeV for the ^{245}Cm(n_{th},f) reaction.

Bearing in mind that the excitation energy of the fragments is higher for heavier actinides due to the steeper increase of the total energy release compared to the total kinetic energy of the fragments, the NEDA fraction would be larger for these nuclides. However, this speculation needs to be verified both experimentally and theoretically. Therefore, the scope of the proposed study should be extended to include minor actinides, not only from an applications point of view, but also in order to understand the observed nuclear physics phenomena.

2.6. Emissive fission domain – Figs. 6 and 7

The phenomenological approach developed by Maslov *et al.* [6, 7, 25, 31] has been extended towards the emissive (multi-chance) fission domain up to E_n = 20 MeV. A similar approach assuming three neutron sources (emissive fission neutrons, emission from fully accelerated fragments and emission from fragments during acceleration) has also been proposed by the Obninsk group [32-34]. Analysis of the measured PFNS for neutron-induced fission of ^{232}Th, ^{235}U, ^{238}U, ^{239}Pu, and ^{237}Np shows that a number of features in the data are correlated with the influence of *(n, xnf)* pre-fission neutron spectra on the PFNS. Consistency has been achieved with extensive LANL/CEA measurements of PFNS and average energy $\langle E \rangle$ for ^{235,238}U and ^{237}Np [35-37]. Calculated energies of the PFNS average energy $\langle E \rangle$ reproduce closely the dips observed in LANL/CEA measurements, representing the opening of a new multi-chance fission channel. Only qualitative consistency with measured $\langle E \rangle$ data is demonstrated in the case of JEFF-3.1 or ENDF/B-VII.0, which is out of phase with (*n, xnf*)-channel openings. The Madland-Nix [9] model calculations of the variation of $\langle E \rangle$ with increase of E_n do not appear to use the correct pre-fission neutron spectra.

3. Recommended Scope

3.1. Nuclides and energy range

The recommend scope is to evaluate prompt fission spectra as a function of neutron energy (ENDF MF5/MT18) from thermal to 20 MeV. The new evaluations should perform equally well in all energy regions: thermal, fast (0.5-2 MeV) and emissive fission (above 4-6 MeV) regions. Highest priority is for the major actinides ^{235,238}U and ^{239}Pu, although we also recommend inclusion of ^{233}U and ^{232}Th along with important minor actinides like ^{237}Np, ^{241}Am, ^{240}Pu and ^{245}Cm if resources permit.

3.2. Covariances

An important goal would be to provide not just recommended spectra, but also an assessment of the uncertainties and correlations (ENDF MF35/MT18 covariance data). These uncertainties should reflect the uncertainties in the experimental data, model parameters, and models.

3.3. Theory and model development

There are a number of different theoretical and phenomenological approaches to evaluating the spectra, for example the traditional Madland-Nix/Los Alamos model [9], refinements to the Los Alamos model [10, 11] (as employed in JENDL), and the methods of Kornilov/Maslov [5-7, 25, 31]. Open questions exist, such as the possible existence of scission neutrons (and/or neutrons emitted during fragment acceleration), or angular anisotropy of neutron emission in center-of-mass system as envisaged by Terrell [38]. These problems should be further studied. At energies above 5-10 MeV incident energy, preequilibrium processes should be included. An important question is the interpretation of the higher spectra values at low emission energies (below 1 MeV outgoing energy) seen in some older experiments and confirmed in recent data, for example, by postulating different temperatures for the light and heavy fragments prior to full acceleration (as in the Kornilov *et al.* [5] approach). These questions can also be investigated by the explicit detailed fragment decay models, as in the TALYS and LANL Monte-Carlo sequential decay codes, as well as by the multi-modal approach presented at this meeting by Ohsawa *et al.*

3.4. Experiments

There is a paucity of measured data. Furthermore, there remain a number of discrepancies in the measurements, as discussed earlier. An important question is whether (as is seen in some data sets) the fission spectrum is higher for low emission energies below 1 MeV – as accounted for by the Maslov/Kornilov formulations, but not in the ENDF/B-VII, JENDL, and JEFF databases for ^{235}U and ^{239}Pu. On the other hand, these higher-value emission energy spectrum data below 1 MeV of outgoing energy may be an artefact arising from experimental problems (is the ^{235}U low-energy behaviour of Madland-Nix evaluations from thermal – fast incident neutron energies driven by matching the Johansson data at 0.5 MeV, for example, which are not matched by Kornilov/Maslov calculations ?) New experimental results shown at this meeting tend to confirm the higher probability of neutron emission below 1 MeV of emission energy as shown in Starostov *et al.* data [16].

Additional experiments are required to help resolve these questions. Furthermore, in some cases (e.g. ^{235}U thermal fission), the feedback from dosimetry threshold reaction data testing for emission energies above 5 MeV appears to contradict the differential spectrum measurements. We note some on-going experimental programmes that should play an important role: (1) when finalized, JRC measurements at Budapest for ^{235}U thermal will be valuable – and will be of even more value if they can be extended down to 0.1 MeV emitted neutron energy; (2) new Gatchina data at thermal energy will also be useful because they extend down to 200 keV, and the energy-angle distributions would help understand the possible role of scission neutrons; (3) JRC measurements for 0.5 MeV on ^{235}U are of interest – more work is needed to understand the angular variations – possible B-III/CEA follow-up experiments at 0.5 MeV to confirm these data will be of interest; (4) LANL-LLNL-CEA programme at LANSCE to upgrade the FIGARO detector should provide valuable data. There is a goal to extend the emission spectra range down below 1 MeV, and up above 8 MeV with much better statistics.

There are several experimental PFNS data sets which are not currently available in the EXFOR database. We would like to compile into EXFOR all existing experimental data including measurements reported in laboratory reports and conferences, but never published in journals.

3.5. Validation

Validation should be an integral part of the evaluation process – an iterative approach is needed to take into account as much information as possible that includes both differential cross-section and spectra measurements, and integral criticality and dosimetry data. However, validation testing represents a challenge since some of the key observables, such as k_{eff} also depend on other nuclear data such as inelastic neutron cross sections and angular distributions, capture, etc. Sensitivity studies to these differing quantities can help disentangle the various contributions. Dosimetry testing of reaction rates involving many different reactions with differing threshold provides a very valuable test. Such work has been pioneered by Mannhart [39] and extended by the IAEA neutron cross-section standards group, the IRDF community for ^{235}U thermal cross sections, and by LANL for fast ^{235}U and ^{239}Pu systems - more work is needed in this area. Finally we also note that the simulations of the spectral index for ^{238}U(n,f)/^{235}U(n,f) (which can be thought of as measuring the fraction of neutrons above ~1 MeV) in Godiva and Jezebel critical assemblies have shown a few-percent under-prediction in the spectral index C/E using ENDF/B-VII evaluations – this discrepancy needs to be resolved. Other nuclear data may need to be improved, although (for example) in ^{239}Pu the ENDF/B-VII total inelastic scattering exceeds that of JEFF3.1 and Maslov *et al.* [40] at E_n=0.5 MeV by ~30% and this might impact the calculated spectral index. The total inelastic cross-section evaluations for ^{235}U in these databases exhibit closer similarity. Another outstanding discrepancy is for some ^{239}Pu solution critical assemblies, for which k_{eff} is over-predicted by about 0.6% on average in ENDF/B-VII and JEFF3.1 – perhaps a new fission spectrum at thermal energy (see Fig. 4), which is used as a normalization point for higher incident neutron energies in [25], could help solve this problem.

4. Conclusions

A new IAEA CRP on prompt fission neutron spectra evaluations is strongly recommended by meeting participants. The main proposed goal would be to determine the prompt fission neutron spectra and covariance matrices for actinides in the energy range from thermal to 20 MeV, including validation against integral critical assembly (k-eff) and dosimetry data.

The following nuclei should be considered in the following order of priority:

- major actinides ^{235,238}U and ^{239}Pu;
- ^{232}Th and ^{233}U of relevance to the Th-U fuel cycle;
- minor actinides such as ^{237}Np, ^{241}Am, ^{242m}Am, ^{240}Pu and ^{245}Cm.

REFERENCES

[1] CHADWICK, M.B., OBLOZINSKY, P., HERMAN, M., *et al.*, ENDF/B-VII.0: Next generation evaluated data library for nuclear science and technology, Nucl. Data Sheets **107** (2006) 2931-3060 (available at http://www.nndc.bnl.gov/).

[2] ROMAIN, P., MORILLON, B., *et al.*, JEFF-3.1, 2005 (available at http://www.nea.fr/).

[3] SHIBATA, K., KAWANO, T., NAKAGAWA, T., *et al.,* Japanese Evaluated Nuclear Data Library Version 3 Revision-3: JENDL-3.3, Nucl. Sci. Technol. **39** (2002) 1125-1199.

[4] Russian File of Evaluated Neutron Data RUSFOND, Obninsk, Russia, 2006 (available at http://www.ippe.ru/podr/abbn/libr/rosfond.php).

[5] KORNILOV, N.V., KAGALENKO, A.B., HAMBSCH, F.-J., Calculation of the prompt fission neutron spectra on the basis of new systematic of the experimental data, Phys. At. Nucl. **62** (1999) 209-220.

[6] MASLOV, V.M., PORODZINSKIJ, Yu.V., BABA, M., *et al.*, Prompt fission neutron spectra of ^{238}U and ^{232}Th above emissive fission threshold, Phys. Rev. **C69** (2004) 034607.1-14.

[7] MASLOV, V.M., KORNILOV, N.V., KAGALENKO, A.B., *et al.*, Prompt fission neutron spectra of ^{235}U above emissive fission threshold", Nucl. Phys. **A760** (2005) 274-302.

[8] IWAMOTO, O., NAKAGAWA, T., OTSUKA, N., CHIBA, S., OKAMURA, K., CHIBA, G., Development of JENDL Actinoid File, paper presented at Int. Conf. on Reactor Physics, Nuclear Power: a Sustainable Resource, PHYSOR 2008, 14-19 September 2008, Interlaken, Switzerland; Nucl. Data Sheets **109** (2008) 2885-2889 (available online at http://wwwndc.jaea.go.jp/ftpnd/jendl/jendl-ac-2008.html).

[9] MADLAND, D., NIX, J., New calculation of prompt fission neutron spectra and average prompt neutron multiplicities, Nucl. Sci. Eng. **81** (1982) 213-271.

[10] OHSAWA, T., HORIGUCHI, T., HAYASHI, H., Multimodal analysis of prompt neutron spectra for ^{237}Np(n,f), Nucl. Phys. **A653** (1999) 17-26.

[11] OHSAWA, T., HORIGUCHI, T., MITSUHASHI, M., Multimodal analysis of prompt neutron spectra for ^{238}Pu(sf), ^{240}Pu(sf), ^{242}Pu(sf) and ^{239}Pu(n_{th},f), Nucl. Phys. **A665** (2000) 3-12.

[12] JOHANSSON, P.I., HOLMQVIST, B., WIEDLING, T., An experimental study of the prompt fission neutron spectrum induced by 0.5 MeV incident neutrons on U-235, Nucl. Sci. Eng. **62** (1977) 695-708; EXFOR 20175.

[13] MASLOV, V.M., PORODZINSKIJ, Yu.V., BABA, M., HASEGAWA, A., KORNILOV, N.V., KAGALENKO, A.B., TETEREVA, N.A., Evaluation of PFNS for U-235, unpublished, 2008 (available online at http://www-nds.iaea.org/minskact).

[14] BOYKOV, G.S., DMITRIEV, V.D., KUDYAEV, G.A., OSTAPENKO, Yu.B., SVIRIN, M.I., SMIRENKIN, G.N., Neutron spectrum in the fission of Th-232, U-235 and U-238 by neutron with energies 2.9 and 14.7 MeV, Phys. At. Nuclei **53** (1991) 392; Yad. Fiz. **53** (1991) 628-648; EXFOR 41110.

[15] WEIGMANN, H., HAMBSCH, F.-J., MANNHART, W., BABA, M., TINGJIN, L., KORNILOV, N., MADLAND, D., STAPLES, P., Fission neutron spectra of U-235, Report WPEC SG9: A report by the Working Party on International Evaluation Co-operation of the NEA Nuclear Science Committee, Volume 9, OECD, Paris, 2003.

[16] STAROSTOV, B.I., NEFEDOV, V.N., BOYCOV, A.A., Prompt neutrons spectra from the thermal neutron fission of U-233, U-235, Pu-239 and spontaneous fission of Cf-252 in the secondary neutron energy range 0.01 - 12 MeV, Vop. At. Nauki i Tekhn., Ser.Yad. Konstanty **3** (1985) 16; EXFOR 40930;
High precision prompt neutron spectra measurements for neutrons from Cf-252, U-233, U-235, Pu-239 fission in the energy range 2-11 MeV, pp. 290-293 in Proc. All Union Conf. on Neutron Physics, 2-6 October 1983, Kiev, Moscow, 1984. (in Russian); EXFOR 40872.

[17] YUFENG, W., BAI XIXIANG; LI ANLI; WANG XIAOZHONG; LI JINGWEN, *et al*., Experimental study of the prompt neutron spectrum of ^{235}U fission induced by thermal neutrons, Chin. J. Nucl. Phys. **11** (1989) 47-54 (see Ref. [15] for numerical data).

[18] LAJTAI, A., KECSKEMETI, J., SAFAR, J., DYACHENKO, P.P., PIKSAIKIN, V.M., Prompt neutron spectra for energy range 30 keV - 4 MeV from fission of U-233, U-235 and Pu-239 induced by thermal neutrons, pp. 312-315 in Proc. advisory group meeting, 12-16 November 1984, JRC-EC, Geel, Belgium, IAEA-TECDOC-335, IAEA, Vienna, Austria, 1984; EXFOR 30704.
Energy spectrum measurements of neutrons for energies 30 keV – 3 MeV from thermal fission of main fuel elements, pp. 613-616 in Proc. Int. Conf. Nuclear Data for Basic and Applied Sciences, 13-17 May 1985, Santa Fe, NM, USA, YOUNG, P.G., BROWN, R.E., AUCHAMPAUGH, F., LISOWSKI, P.W., STEWART, L. (Eds), Gordon and Breach, New York, USA, 1986, Vol.1; EXFOR 30704.

[19] KORNILOV, N.V., HAMBSCH, F.-J., FABRY, I., OBERSTEDT, S., SIMAKOV, S.P., JRC IRMM NP Scientific Report 2007, Report EUR 23440EN (2008) 28.

[20] TRUFANOV, A.M., LOVCHIKOVA, G.N., SMIRENKIN, G.N., POLYAKOV, A.V., VINOGRADOV, V.A., Measurements and estimates of the average energy of neutrons from the U-236(n,f) reaction, Phys. At. Nucl. **57** (1994) 572-578; Yad. Fiz. **57** (1994) 606-613; EXFOR 41162.

[21] STAPLES, P., EGAN, J.J., KEGEL, G.H.R., MITTLER, A., WOODRING, M.L., Prompt fission neutron energy spectra induced by fast neutrons, Nucl. Phys. **A591** (1995) 41-60; EXFOR 13982.

[22] YOUNG, P.G., CHADWICK, M.B., MACFARLANE, R.E., TALOU, P., KAWANO, T., MADLAND, D.G., WILSON, W.B., WILKERSON, C.W., Evaluation of neutron reactions fro ENDF/B-VII: $^{232\text{-}241}$U and ^{239}Pu, Nucl. Data Sheets **108** (2007) 2589-2654.

[23] NEFEDOV, V.N., STAROSTOV, B.I., BOJTSOV, A.A., High precision spectra measurements for neutrons arising from the fission of Cf-252, U-233, U-235, Pu-239 in the energy range 0.04 - 5 MeV, pp. 285-289 in Proc. All Union Conf. on Neutron Physics, 2-6 October 1983, Kiev, Moscow, 1984. (in Russian); EXFOR 40871.

[24] BOJTSOV, A.A., SEMENOV, A.F., STAROSTOV, B.I., Relative measurements of the spectra of prompt fission neutrons for thermal neutron fission of the nuclei U-233, U-235, Pu-239 in the energy range 0.01 - 5 MeV, pp. 294-297 in Proc. All Union Conf. on Neutron Physics, 2-6 October 1983, Kiev, Moscow, 1984. (in Russian); EXFOR 40873.

[25] MASLOV, V.M. ^{239}Pu prompt fission neutron spectra, Atomic Energy **103** (2007) 633-640.

[26] SUKHIKH, S.E., LOVCHIKOVA, G.N., VINOGRADOV, V.A., ZHURAVLEV, B.N., SAL'NIKOV, O.A., MERTENS, H., RUBEN, A., Spectra of the fission prompt neutrons arising at the interaction of 1.5-MeV neutrons with U-235 nucleus, Atomnaya Energiya **69** (1990) 28-31; EXFOR 41144.

[27] DRAPCHINSKY, L.V., *et al.*, Prompt fission neutron spectra of Cm-245(n,th) reaction, Project technical report ISTC 183B-96, unpublished, 1999. Numerical data provided by the Nuclear Data Center, Japanese Atomic Energy Agency (JAEA).
[28] WANG FU-CHENG, HU JI-MIN, A study of the multimode fission model, J. Phys. G **15** (1989) 829-848.
[29] BELGYA, T., BERSILLON, O., CAPOTE, R., FUKAHORI, T., ZHIGANG, G., GORIELY, S., HERMAN, M., IGNATYUK, A.V., KAILAS, S., KONING, A., OBLOZINSKY, P., PLUJKO, V., YOUNG, P., Handbook for calculations of nuclear reaction data, RIPL-2, IAEA-TECDOC-1506, IAEA, Vienna, 2006 (available online at http://www-nds.iaea.org/RIPL-2/).
[30] MASLOV, V.M., SOUKHOVITSKI, E., PORODZINSKIJ, Yu.V., *et al.*, Evaluation of neutron data for Curium-245, report INDC(BLR)-003, IAEA, Vienna, 1996.
[31] MASLOV, V.M., Prompt fission neutrons spectra of ^{238}U, Phys. At. Nucl. **71** (2008) 9-26; Yad. Fiz. **71** (2008) 11-27).
[32] LOVCHIKOVA, G.N., SMIRENKIN, G.N., TRUFANOV, A.M., *et al.*, Energy distributions of secondary neutrons from the neutron-induced fission of Th-Pu nuclei, Phys. At. Nucl. **62** (1999) 1460-1468; Yad. Fiz. 62 (1999) 1551-1561.
[33] SVIRIN, M.I., TRUFANOV, A.M., Average energy of prompt fission neutrons of ^{235}U for incident neutron energies below 20 MeV, Yad. Fiz. **70** (2007) 656-670 (in Russian).
[34] SVIRIN, M.I., Spectral shape and average energy of prompt fission neutrons of ^{237}Np for incident neutron energies below 20 MeV, Yad. Fiz. **71** (2008) 1725-1741 (in Russian).
[35] ETHVIGNOT, T., DEVLIN, M., DROSG, R., GRANIER, T., HAIGHT, R.C., MORILLON, B., NELSON, R.O., O'DONNEL, J.M., ROCHMAN, D., Prompt fission neutron average energy for ^{238}U(n, f) from threshold up to 200 MeV, Phys. Lett. **B575** (2003) 221-227.
[36] ETHVIGNOT, T., DEVLIN, M., DUARTE, H., GRANIER, T., HAIGHT, R.C., MORILLON, B., NELSON, R.O., O'DONNEL, J.M., ROCHMAN, D., Neutron multiplicity in the fission of ^{238}U and ^{235}U with neutrons up to 200 MeV, Phys. Rev. Lett. **94** (2005) 052701-4.
[37] TAIEB, J., GRANIER, T., ETHVIGNOT, T., DEVLIN, M., HAIGHT, R.C., *et al.*, Measurement of the average energy and multiplicity of prompt fission neutrons from ^{237}Np(n, f) from 0.7 to 200 MeV", pp. 429-432 in Proc. Int. Conf. on Nuclear Data for Science and Technology, 22-27 April 2007, Nice, France, BERSILLON, O., GUNSING, F., BAUGE, E., JACQMIN, R., LERAY, S. (eds.), EDP Sciences, France, 2007.
[38] TERRELL, J., Fission neutron spectra and nuclear temperatures, Phys. Rev. **113** (1959) 527-541.
[39] MANNHART W., In: International Neutron Cross-Section Standards: Measurements and Evaluation Techniques Summary Report of Consultant's Meeting, 13 - 15 October 2008, Rep. INDC(NDS)-0540 (IAEA, Vienna, 2008) , p.15.
[40] MASLOV, V.M., OBLOZINSKY, P., HERMAN, M., Review and Assessment of Neutron Cross Section and Nubar Covariances for Advanced Reactor Systems, Rep. BNL- 81884-2008-IR (Brookhaven, NY, USA, 2008).

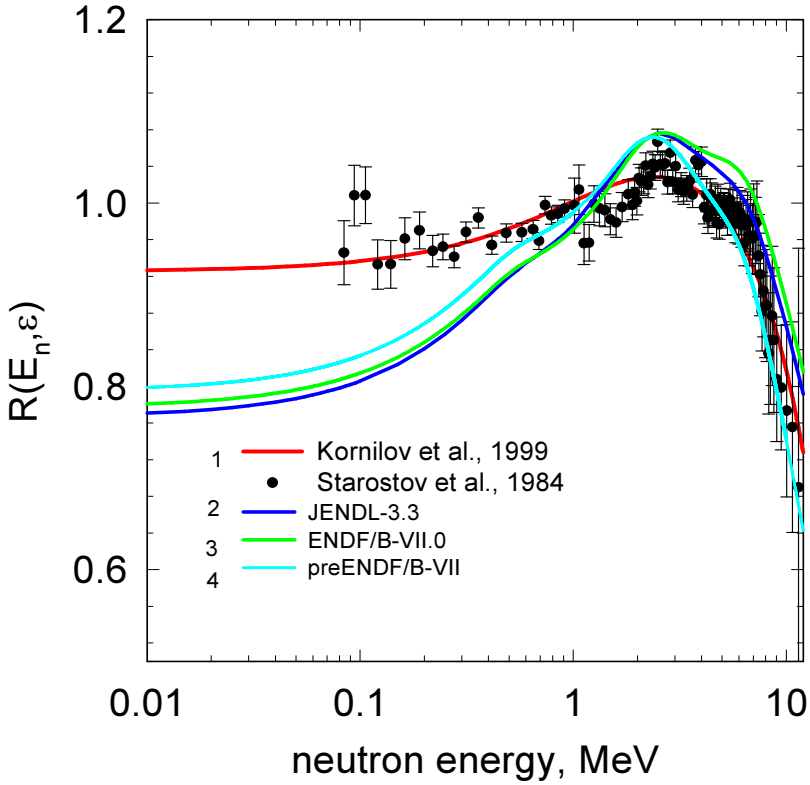

FIG.1a. $^{235}U + n(th)$*: Ratio of PFNS to the Maxwellian distribution at fixed temperature in logarithmic energy scale.*

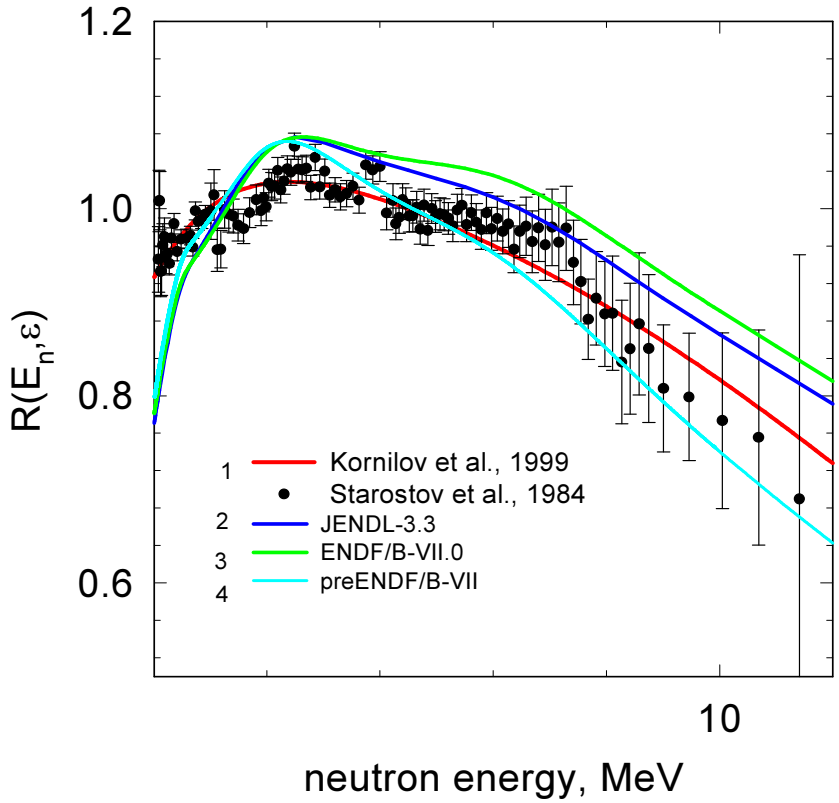

FIG.1b $^{235}U + n(th)$*: Ratio of PFNS to the Maxwellian distribution at fixed temperature in linear energy scale.*

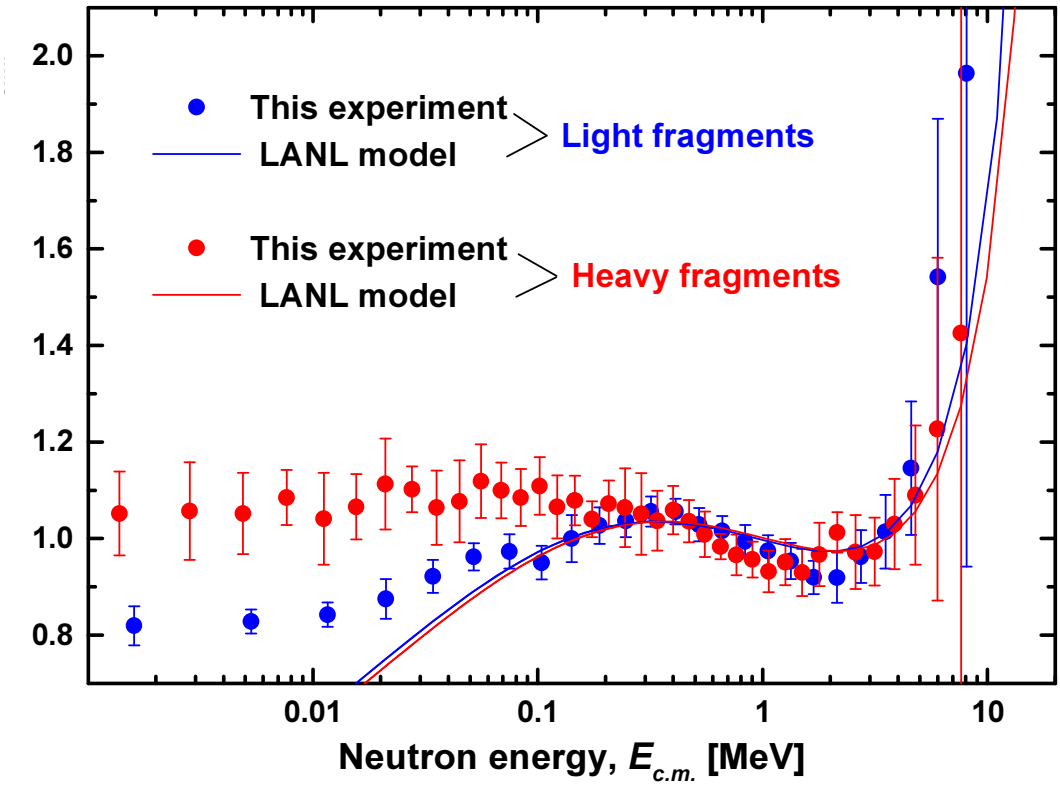

FIG. 2. ^{235}U *+ n(th): Ratio of PFNS in the CM system to the Maxwellian distribution at fixed temperature* T_{light} *= 0.78 MeV and* T_{heavy} *= 0.84 MeV. Measured data presented by Vorobyev et al. at this meeting; Madland-Nix model with constant inverse cross-sections used.*

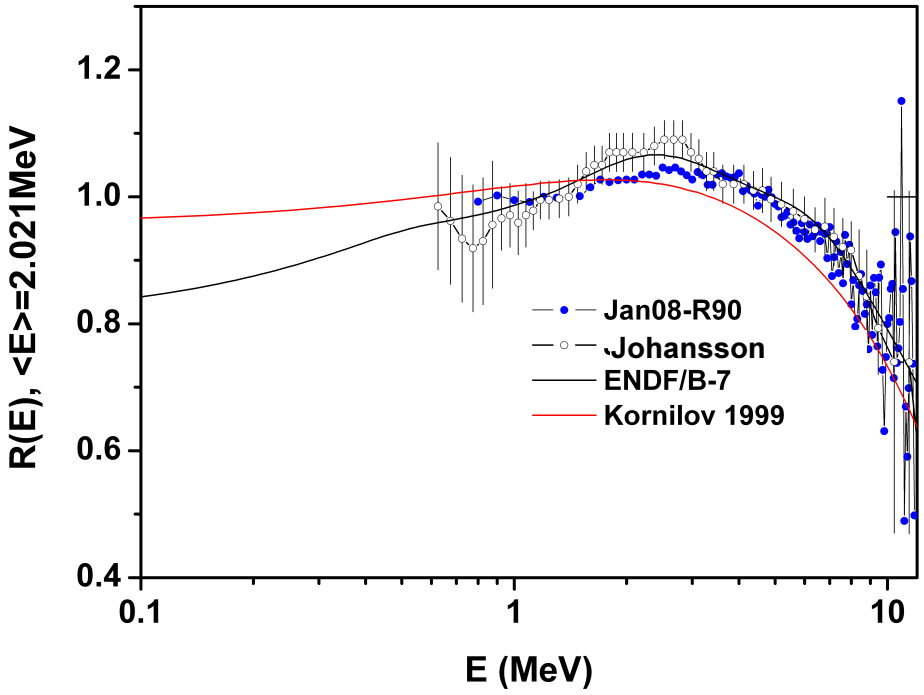

FIG. 3. ^{235}U *+ n (0.5MeV): JRC new measurements compared with Johansson et al. [12] measurements, Kornilov et al. (1999) parameterization [5] and ENDF-B/VII evaluation.*

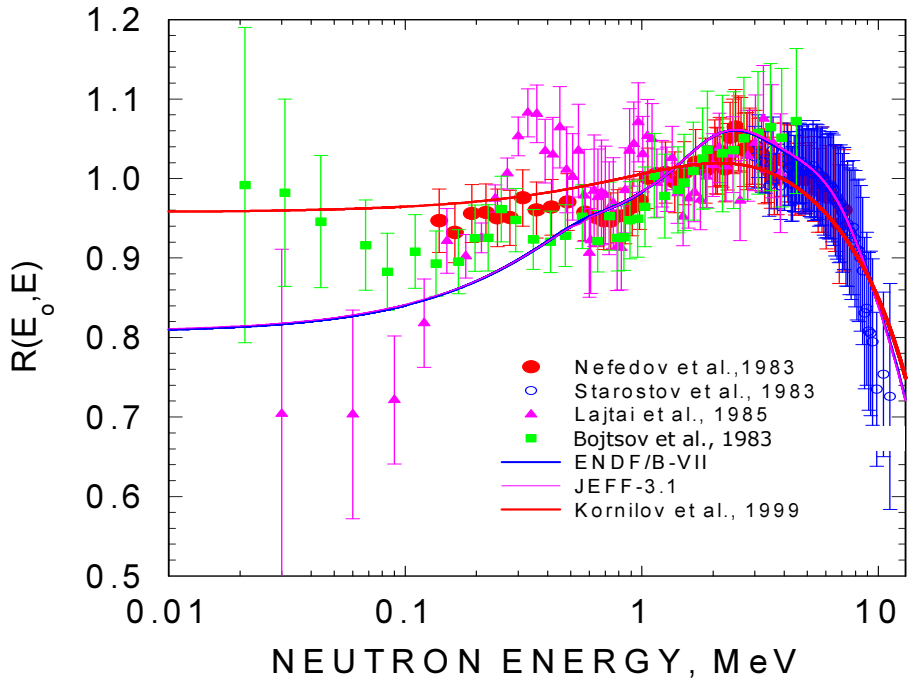

FIG. 4. ^{239}*Pu + n(th): Ratio of PFNS to the Maxwellian distribution at fixed temperature.*

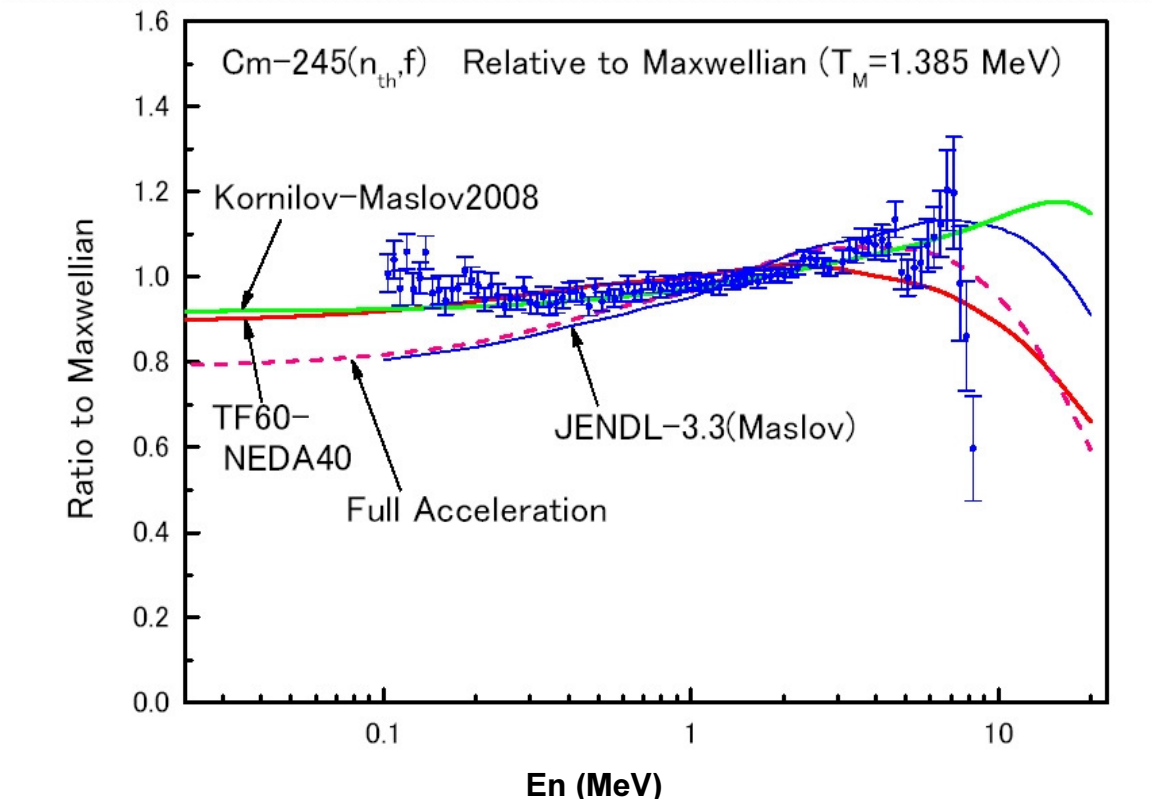

FIG. 5. ^{245}*Cm + n(th): Ratio of PFNS to the Maxwellian distribution at fixed temperature.*

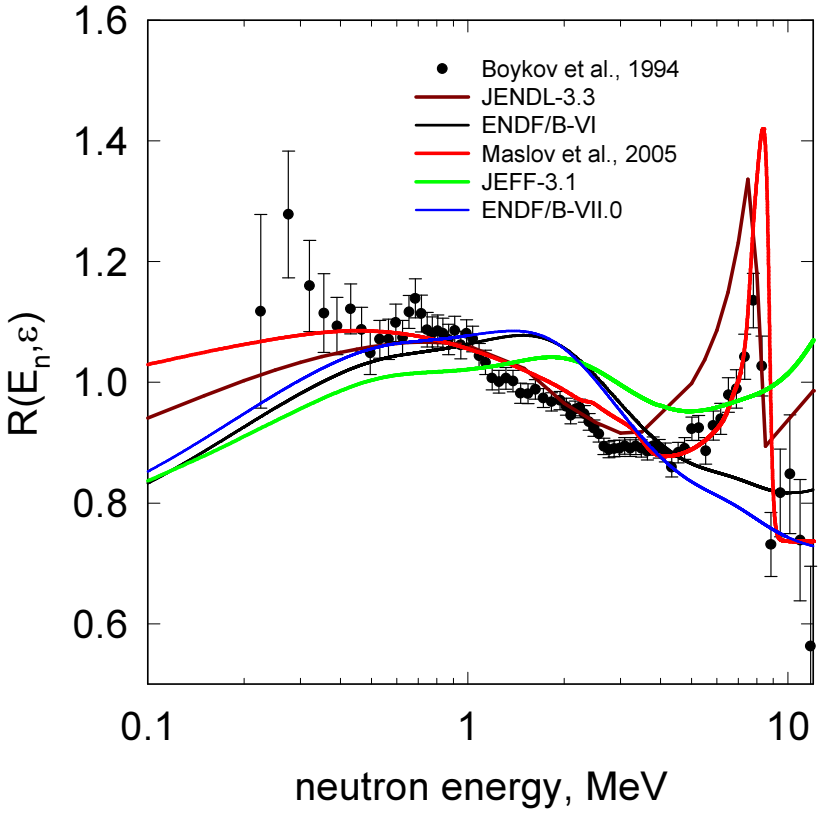

FIG. 6. ^{235}U + n(14 MeV) *in the emissive fission domain.*

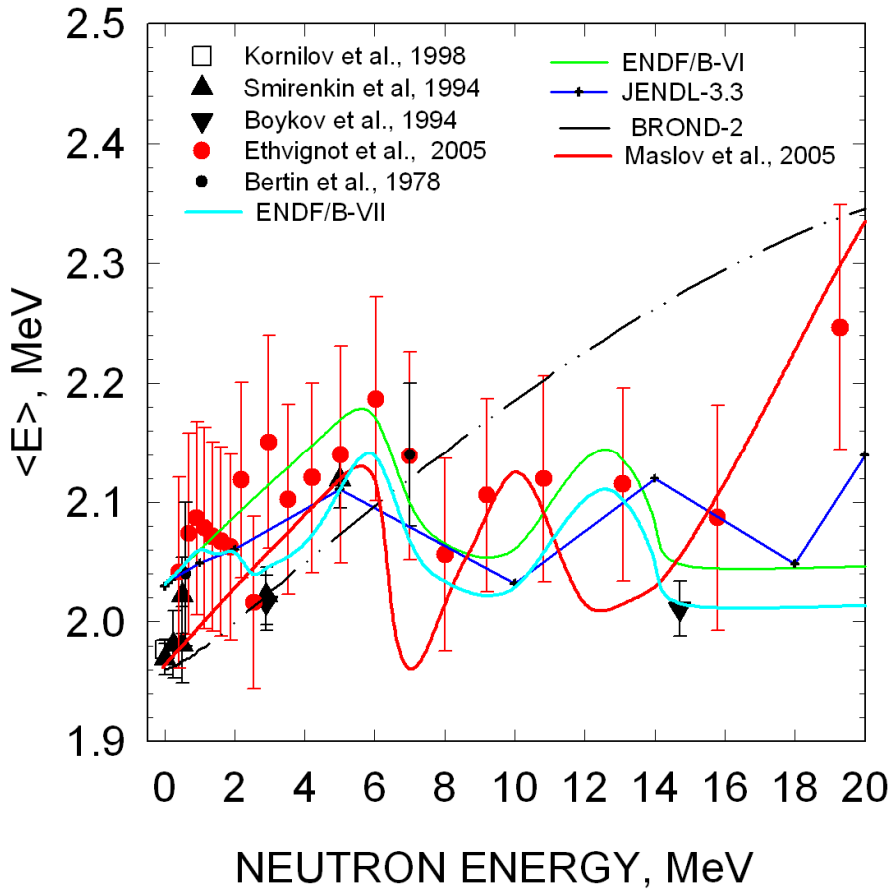

FIG. 7. $n + ^{235}U$: *Average energy of PFNS vs incident neutron energy.*

Consultants' Meeting on

"Prompt Fission Neutron Spectra of Major Actinides"

IAEA Headquarters, Vienna, Austria
24 – 27 November 2008

Meeting Room B0404

Provisional AGENDA

Monday, 24 November

08:30 - 09:15	**Registration** (IAEA Registration desk, Gate 1)
09:30 - 10:00	**Opening Session**
	Welcoming address – Alan L. Nichols
	Introductory Remarks – Roberto Capote Noy
	Election of Chairman and Rapporteur
	Adoption of Agenda
10:00 - 12:30	**Session 1: Presentations by participants**
	M.B. Chadwick
	E. Bauge
	T. Ohsawa
12:30 – 14:00	***Lunch***
14:00 – 18:00	**Session 1 cont'd: Presentations by participants**
	A. Vorobyev
	V. Maslov
	S. Oberstedt
	Coffee break as needed
19:00	***Dinner at Restaurant in the City***

Tuesday, 25 November

09:00 - 18:00	**Session 2: Discussion on CRP goals and outcomes**
	Coffee breaks and lunch break in between

Wednesday, 26 November

09:00 - 12:30	**Session 2 cont'd: Discussion on CRP goals and outcomes**
	Coffee break as needed
12:30 – 14:00	***Lunch***
14:00 – 17:00	**Session 3: Preparation of report and recommendations**

Thursday, 27 November

09:00 - 12:30	**Session 3 cont'd: Finalisation of report and recommendations**
	Coffee break as needed
12:30	**Closing of the meeting**

Consultants Meeting on
"Prompt fission neutron spectra of major actinides"

IAEA Headquarters, Vienna, Austria
24 to 27 November 2008

LIST OF PARTICIPANTS

BELARUS

Vladimir Maslov
Joint Institute for Power and
Nuclear Research-Sosny
99 Academician
A.K. Krasin Str.
Minsk BY-220109
Tel. +375 17 2994441
Fax +
e-mail: maslov@bas-net.by

FRANCE

Eric Bauge
DPTA/SPN
CEA/DIF
B.P. No. 12
91680 Bruyeres-le-Chatel
Tel. +33
Fax +33
e-mail: eric.bauge@cea.fr

JAPAN

Takaaki Ohsawa
Department of Nuclear Engineering
Faculty of Science and Technology
Kinki University
3-4-1 Kowakae
Higashi-Osaka-shi
Osaka-fu 577-8502
Tel. +81 6 6730 5880
Fax +
e-mail: ohsawa@ele.kindai.ac.jp

RUSSIA

Alexander Vorobyev
Petersburg Nuclear Physics Institute
Orlova Roscha
188300 Gatchina
Leningrad Region
Tel. +
Fax +
e-mail: alexander.vorobyev@pnpi.spb.ru

USA

Mark B. Chadwick
Group T-2, MS-B243
Theoretical Division
Los Alamos National Laboratory
Los Alamos, NM 87545
Tel. +1 505 667 9671
Fax +1 505 667 9671
e-mail: mbchadwick@lanl.gov

INTERNATIONAL ORGANIZATION

Stephan Oberstedt
EC-JRC-IRMM
Retieseweg
2440 Geel
Belgium
Tel. +
Fax +
e-mail: stephan.oberstedt@ec.europa.eu

IAEA

Roberto Capote Noy
Nuclear Data Section
Division of Physical and Chemical Sciences
Tel. +43-1-2600-21713
Fax +43-1-26007
e-mail: r.capotenoy@iaea.org

Multimodal Madland-Nix Model: Stick to Physics or Go *ad hoc* Fitting?

Takaaki Ohsawa
Faculty of Science and Engineering, Kinki University, Higashi-osaka, Japan

1. Introduction

Early representations of the prompt fission neutron spectrum (PFNS) include Maxwellian and Watt[1] spectrum, with single and two parameter(s), respectively, adjusted so as to reproduce the experimental data. These formulas, however, involve poor physics, because they neglect the diversity in the excitation energy, the shell effects on the properties of fission-fragments (FFs), and also the neutron transmission coefficients which undoubtedly affect the neutron emission probability.

Efforts have been paid in the last twenty-five years to give better description of the physics of the prompt neutron emission. These efforts are categorized into four groups[2] : (A) Simplified temperature distribution model (*e.g.*, Madland-Nix[3]), (B) Cascade evaporation model (*e.g.*, Märten-Seeliger[4], Hu-Wang[5]), (C) Hauser-Feshbach model (*e.g.*, Browne-Dietrich[6], Gerasimenko *et al.*[7]), (D) Monte Carlo method (*e.g.*, Dostrovsky *et al.*[8] , Lemaire *et al.*[9]) With application to nuclear data evaluation in mind, we applied three criteria for choosing an adequate model: (1) the model should be *accurate,* (2) *not too complicated* and (3) have *predictive power*, because evaluation works often involve prediction of the spectra for nuclides for which no data exist. From these points of view, we chose the Madland-Nix (M-N) model as a basis of the present methodology.

2. Refinements on the Madland-Nix Model

Another important point is that the methodology should be grounded on the present knowledge of fission physics and should be consistent with it. At present, the most successful and consistent description[10] of the partition of mass and energy, and even the dispersion of the total kinetic energy (TKE) as a function of FF mass, is provided by multimodal random neck-rupture (MM-RNR) model. This model, originally proposed by Brosa *et al.*[11], has been applied to analyze the data of many fissioning systems, and is also consistent with the results of other theoretical approaches such as scission point model[12] and Hartree-Fock-Bogoliubov calculations[13]. The model was incorporated into the code *talys* together with relevant systematics to analyze the fission cross sections and FF mass distributions[14]. The present author[15, 16] was the first to propose to incorporate the MM-RNR model into the M-N model to consider the variety in mass and excitation energy distributions of FFs as well as other refinements. The proposed refinements include the following points:

(1) *Multimodal fission process*: Spectra for each mode (standard-1 (S1), standard-2 (S2), superlong (SL) modes for $^{235}U(n_{th},f)$) were calculated separately, because the total excitation energy (TXE) distributions and level density parameters (LDP) for typical FFs differed greatly depending on the modes (Fig.1). Calculation showed that the S1-spectrum was the softest, the SL-spectrum the hardest, with the S2-spectrum coming in between (Fig.2). The total spectrum from multimodal calculation tended to be softer than the conventional single-modal spectrum, because of the contribution of softer S1-component.

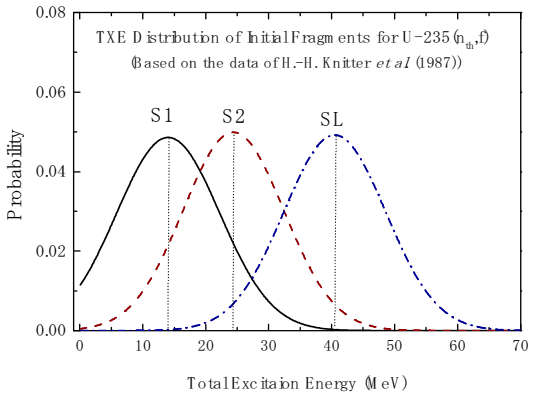

Fig.1 Initial TXE distributions for ^{235}U(n_{th},f)

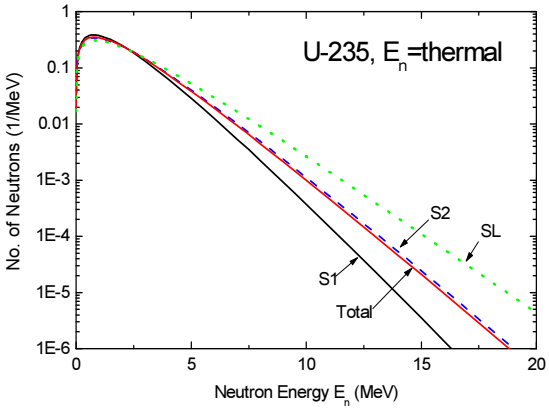

Fig. 2 Modal spectra for ^{235}U(n_{th},f)

(2) *Level Density Parameters*: In the present approach, the LDPs were obtained by numerically solving the transcendental equation of Ignatyuk[17],

$$a(U) = \tilde{a}(A)[1 + f(U)\delta W / U], \quad f(U) = 1 - \exp(-\gamma U), \quad U = at^2$$

instead of the simple relation $a=A/$C used in the original M-N model. As Fig.3 shows, the measured LDPs for FFs show a marked saw-toothed structure due to strong shell effects around A≈132, which is well reproduced by the Ignatyuk model. The linear approximation $a=A/10$ represents just the asymptotic value $\tilde{a}(A)$ in eq. (1) in the limit of no shell correction (δW=0). Sensitivity analysis (Fig.4) has shown that **the high-energy part of the spectrum is very sensitive to the LDP but the low-energy part is not**. A critical test[18] on ^{242m}Am(n_{th},f) showed that the present method, without any *ad hoc* adjustment, gave excellent agreement with the experiment[19] up to emitted neutron energy 14 MeV. This proves the fact that the present method, *esp*. the LDPs used, is physically correct.

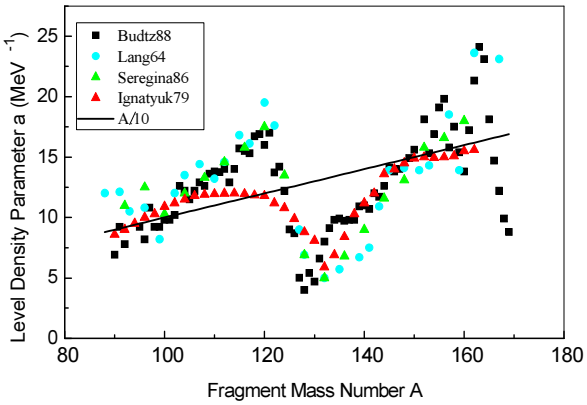

Fig. 3. Calculated and experimental LDPs for FF.

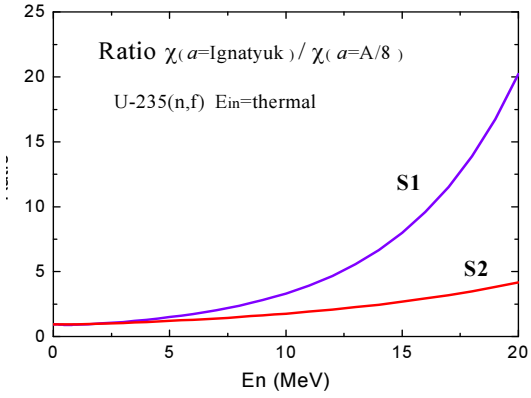

Fig. 4. Sensitivity of the spectrum to the LDP.

(3) *Asymmetry in neutron multiplicity from light and heavy fragments*

It has been common practice to simply average the spectra from light fragment (LF) and heavy fragment (HF) to obtain the total spectra, assuming implicitly that an equal number of neutrons are emitted from the two fragments. However, this is not always the case, since the excitation energies of the two FFs are not always equal. Therefore a weighted average should be taken instead. This should be emphasized all the more because spectral shapes from LF and HF are very different (Fig.5), mainly due to kinematics of the FFs, and partially due to different energy-dependent behavior of the inverse reaction cross sections for LF and HF[18].

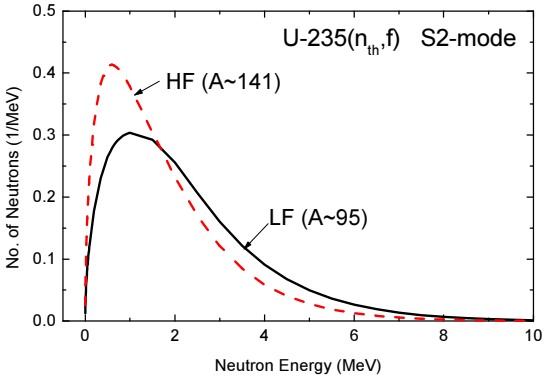

Fig. 5 Laboratory-system spectra from LF and HF.

(4) *Asymmetry in nuclear temperature for LF and HF*

The nuclear temperature T_{L0} and T_{H0} of LF and HF *at the moment of scission* is considered to be equal and small because of large deformation. However, T_L and T_H *at the moment of neutron emission* are not generally equal, because the deformation energies for LF and HF are generally different at scission. So it is reasonable to consider possible difference in the nuclear temperature in the M-N model calculation. Actually, a non-equitemperature M-N model was proposed by the present author at IAEA-CM (1990) [20]. Recently, this idea was taken up again and examined by P. Talou[21] in his Monte Carlo simulation of the PFNS.

3. JENDL-3.3 and JENDL/AC2008

This method has been applied to many actinides and the results were adopted by JENDL-3.3, after integral benchmark testing on fast, thermal and large-leakage benchmark systems, and also with spectrum averaged cross sections[22]. JENDL-3.3 is the only library that includes complete covariance matrices for major actinides, such as ^{233}U, ^{235}U, ^{238}U, ^{239}Pu and ^{240}Pu[23]. These matrices were generated on the basis of sensitivity analysis of the PFNS to input data by the code KALMAN[24]. Evaluations for minor actinides were done by Maslov[25] within the ISTC project, but they were superseded in JENDL/AC2008 by new evaluations using the new code CCONE[26] and multimodal M-N model, because of peculiar fluctuations in his spectra[18].

The criticism that JENDL-3.3 does not adequately reproduce the average neutron energy at 6 MeV is due to the fact that spectral data were given only at 5-MeV interval in the file. The fact is that linear interpolation between 5- and 10-MeV values gave higher average neutron energy. This problem has already been resolved by giving evaluated data at 1-MeV interval. So the alleged 'defect' in JENDL-3.3 is not due to the evaluation method, but merely *a matter of file making*.

Some people criticize that the multimodal M-N approach involves many adjustable parameters. But this is **completely due to ignorance**. On the contrary, **the number of adjustable parameters in this approach is only one**, because the LDPs, which used to be an adjustable parameter in the original M-N model, were uniquely fixed by solving the Ignatyuk equation[17]. Other physical quantities, such as the average mass, TKE of the FFs for each mode, determined from experiments[10], or from systematics[27], were used as inputs **without any change**. Therefore these physical quantities work as **constraints** to the problem, and by no means as free parameters, in the sense that unphysical data of the crucial physical quantities would result in wrong spectra. The only adjustable parameter in our model is the nuclear temperature ratio T_L/T_H. Our method provides a complete prescription for evaluation, according to which even twenty-year-old student can perform the calculation by following the indicated procedure step by step. No expertise or *ad hoc* adjustment is required.

4. Scission Neutrons and/or Neutron Emission During Acceleration?

It has been known that calculations tend to underestimate the spectrum in the emitted neutron energy region E_n<1. There are three possibilities to explain this: (a) the measured data in the low-energy region are contaminated by scattered neutrons, (b) there are some mechanisms of neutron emission other than neutron emission from fully accelerated FFs, such as neutron emission *during* acceleration (NEDA) and scission neutrons (SCN), and (c) there may be an anisotropy in the neutron emission in the FF centre-of-mass frame. There are different views on the energy spectrum and the fraction of SCN depending on the assumed emission mechanism: if neutrons are evaporated *adiabatically* from a largely deformed nuclear matter, the energy should be low; if neutrons are emitted *non-adiabatically* (dynamically) due to drastic change in the nuclear potential in the neck region of the pre-scission nucleus, the energy should be higher. At present, impartially stated, we do not have enough knowledge to judge which is correct. Therefore the author believes **we should refrain from using the SCN as a convenient tool for fitting to measurements.** On the other hand, our analysis on competition between the time required for full acceleration (~10^{-19} sec) of FFs and the average neutron emission time shows that **there is a fair chance of NEDA in the case of S2-mode**, due to high excitation energy of FFs, while there is no chance of NEDA in the case of S1-mode, due to lower excitation energy. This result suggests that NEDA is a more legitimate process than SCNs.

It should also be noted here that **NEDA and SCN hypotheses exclude each other**, because if SCNs are emitted, the excitation energy of the FF is reduced, which makes the neutron-emission time longer, thus making NEDA less probable.

5. Many Source-term Model

There have been proposals to use plural Maxwellian or Watt terms with different temperatures to represent the total spectrum. A similar attempt has recently been made by Kornilov *et al*.[28] to express the total PFNS with empirical formula with **two** Watt functions plus **two** additional SCN terms of Maxwellian shape, plus an **additional** parameters α that represent the NEDA effect. With increased number of parameters, they asserted they were able to get good fits to experimental data.

However, several questions arise here:

(1) The Watt function is merely a Maxwellian with consideration of FF motion, but without consideration of diversity in the initial excitation and cooling during cascading process. Kornilov *et al.* [28] argue that M-N model spectrum is very sensitive to the inverse cross section and LDP. However, Fig. 20 of Madland's paper[3] has shown that different choice of optical potential does not result in *very* different spectra. With the modern knowledge of optical potential, the inverse reaction cross section can now be calculated with reasonable confidence. (Otherwise, the nuclear data evaluation for FPs using the optical model in many files would be untrustworthy.) Also the LDPs nowadays can be calculated with the Ignatyuk model with confidence. (Otherwise, many nuclear data calculation using the LDP would be unreliable.) Therefore, **rejecting the M-N model for the above reasons does not make sense, nor does it prove that Watt formula is superior to M-N model**.

Apparently, the antiquated Watt representation with fixed functional form needed additional terms that complement its inherent deficiency. So it is questionable whether the SNC parameters[28] obtained by least-squared fitting to experimental data represent real physics or not. Some theoretical calculations surely indicate the possibility of SCN. Then why not adopt these theoretical data, avoiding *ad hoc* fitting?

(2) Kornilov *et al*.[28] stated that "the yields of neutrons from the LF and HF differ insignificantly from the mean value (within 10%)". However, this is not true. Experiments[29,30] showed that **more neutrons are emitted from LFs at 0.5 MeV, and from HFs at higher incident energies** (*e.g.*, ν_L=1.44, ν_H=1.02 at 0.5 MeV, while ν_L=1.48, ν_H=1.71 at 5.55 MeV for ^{235}U(n,f); ν_L=1.59, ν_H=1.14 at 0.5 MeV, while ν_L=1.59, ν_H=1.87 at 5.5 MeV for ^{237}Np(n,f)), and the increase in ν_{tot} is totally accounted for by HF alone at 5.55MeV. These phenomena are explained as due to the shell effects on HF with A≈132 at lower energies and its diminishing at higher energies. In view of the large difference in the spectra from LF and HF (Fig.5), the simple average $0.5[W_{LF}+W_{HF}]$ should be replaced by the weighted average $[\nu_L W_{LF}+\nu_H W_{HF}]/(\nu_L+\nu_H)$ at different energies. This change would inevitably require readjusting the *best tuned* SCN parameters reported by Kornilov *et al*.[28].

(3) Assuming two SCN sources *in addition to* NEDA cannot be justified from physics point of view, as was discussed in Sec. 4.
To increase the number of adjustable parameters is surely a convenient way to get better fits to existing measured data, but it diminishes the physical meaning of the results. To the author's mind, this attempt is essentially **an art of *ad hoc* parameter fitting** to the experimental data, and is not based on, nor does it provide further insight into, the fission physics.

6. Concluding Remarks

Nuclear fission is a phenomenon with great diversity and unity, governed by quantum effects such as shell and pairing effects, as well as by the basic principles of physics in the depths. The existence of a solution to a problem concerned depends on, to which level of solution one looks for. The author's philosophy is just **to stick to physics as much as possible, rather than to go *ad hoc* parameter fitting**. Our target should be to understand the various aspects of fission, including the PFNS and the mass and energy partitions, in a consistent framework of fission physics. The author believes that the multimodal fission model provides a ground to examine the possibility of consistent description of fission phenomena. Scientific discussion should be conducted in reference to objective fact and pertinent physical principles. Fitting for the sake of fitting gets us nowhere. Criticism for the sake of criticism is nothing but diplomacy, not science.

References

1) B. E. Watt, Phys. Rev. **87**, 1037 (1952).
2) T. Ohsawa, JAERI-M 92-027 (1992).
3) D. G. Madland and J.R. Nix, Nucl. Sci. Eng. **81**, 213 (1982).
4) H. Märten, D. Neumann and D. Seeliger, IAEA-TECDOC-335, p.255 (1985).
5) J. M. Hu and Z. S. Wang, Physica Energiae Fortis et Physica Nucleris **3**, 772 (1979).
6) J. C. Browne and F. S. Dietrich, Phys. Rev. **C10**, 2545 (1974).
7) B. F. Gerasimenko and V. A. Rubchenya, Proc. All-Union Conf. on Neutron Physics, p.114 (1980).
8) I. Dostrovsky, Z. Fraenkel and G. Friedlander, Phys. Rev. **116**, 683 (1959).
9) S. Lemaire, P. Talou, T. Kawano, M. B. Chadwick and D. Madland, Phys. Rev. **C72**, 024601 (2005).

10) e.g., H.-H. Knitter, F.-J. Hambsch and C. Budtz-Jørgensen, Z. Naturforsch. **42a**, 786 (1987).
11) U. Brosa, S. Grossmann and A. Müller, Phys. Reports **197** (1990).
12) B.D. Wilkins, E.P. Steinberg and R.R. Chasman, Phys. Rev. **C14**, 1832 (1976).
13) H. Goutte, J.F. Berger, P. Casoli and D. Gogny, Phys. Rev. **C71**, 024316 (2005).
14) M.C. Duijvestijn, A.J. Koning and F.-J. Hambsch, Phys. Rev. **C64**, 014607 (2001).
15) T. Ohsawa, T. Horiguchi and H. Hayashi, Nucl. Phys. **A653**, 17 (1999).
16) T. Ohsawa, T. Horiguchi and M. Mitsuhashi, Nucl. Phys. **A665**, 3 (2000).
17) A. V. Ignatyuk, Sov. J. Nucl. Phys. **29**, 450 (1979).
18) T. Ohsawa and H. Taninaka, Paper presented at PHYSOR'08, Interlaken, Switzerland, 2008.
19) L. V. Drapchinsky et al. ISTC 183B-96 (1999).
20) T. Ohsawa, INDC(NDS)-251, p.71 (1991).
21) P. Talou, Proc. Int. Conf. Nuclear Data Sci. Technol. Nice, France, 2007, p.317 (2008).
22) K. Shibata et al., J. Nucl. Sci. Technol. **39**, 1125 (2002).
23) M. Salvatores (ed.) NEA/WPEC-26 (2008), OECD.
24) T. Kawano, T. Ohsawa and K. Shibata, JAERI-Research 99-009 (1999).
25) V. M. Maslov et al. INDC(BLR)-006 (1996), INDC(BLR)-007 (1997).
26) O. Iwamoto, J. Nucl. Sci. Technol. **44**, 687 (2007).
27) F.C. Wang and J. M. Hu, J. Phys. **G15**, 829 (1989).
28) N.V. Kornilov et al., Phys. At. Nucl. **62**, 209 (1999).
29) R. Müller et al., Phys. Rev. **C29**, 885 (1984).
30) A.A. Naqvi et al., Phys. Rev. **C34**, 218 (1986).

ACTINIDE PROMPT FISSION NEUTRON SPECTRA

V.M. Maslov

Joint Institute of Nuclear and Energy Research,
Krasina str., 99, 220109,Minsk-Sosny, Belarus, maslov@bas-net.by

The energy dependence of the measured prompt fission neutron spectra (PFNS) shapes was modeled for ^{232}Th(n, F), ^{238}U(n, F), ^{235}U(n, F) and ^{239}Pu(n, F) reactions for incident neutron energies from thermal up to 20 MeV. The essence of employed approach in the emissive fission domain is the consistency of exclusive pre-fission neutron spectra and emissive fission chances structure with the measured database. The precise description of the PFNS is obtained for major fissile and fertile nuclides, which urges the problem of consistency of integral benchmarks and differential PFNS average energies of ^{235}U(n, F) to be revisited. The conclusive evidences are revealed for implementation of new evaluations of PFNS for major, as well for minor actinides. For that the use of theoretical approach, proven in case of some major actinides, is justified.

The fast reactor upheaval and possible incineration of minor nuclides in a closed fuel cycle will need an essential improvement of the relevant prompt fission neutron spectra. Among all the minor actinides scarce measured differential data on PFNS are available only for the ^{237}Np(*n, F*) reaction, which is insufficient for model' independent evaluation. The employment of the theoretical approach, well tested in case of neutron-induced fission reaction for ^{232}Th, ^{235}U and ^{238}U targets [1—4] at E_n either below and above emissive (n,xnf) fission threshold, when $x \geq 1$ pre-fission neutrons are emitted, looks feasible in case of neutron-induced fission of minor actinides. In the same manner were recently predicted PFNS for ^{239}Pu(*n, F*) [5, 6], soon they would be investigated experimentally in a wide incident neutron energy range by LANL (USA) and CEA (France) collaboration [7, 8].

For ^{235}U(*n, F*) reaction major controversy at present still exists in the PFNS at thermal energies. Usually it is claimed to be due to inconsistencies in measured PFNS data [9, 10, 11]. However, partly the well-known problem of inconsistency of integral thermal data testing and differential data [12] might be attributed to the poor fits of differential PFNS data, which are employed in ENDF/B-VII.0 [12] or JENDL-3.3 [13] data libraries. Figures 1a, 1b show the comparison of measured PFNS data by Starostov et al. [9] with evaluations and phenomenological approach developed by Kornilov et al. [14]. PFNS of [12, 13] are calculated with the Madland-Nix model [15,16] and are claimed to perform better in integral data testing of thermal systems [12]. However, the predicted in [14] increase of soft prompt fission neutrons as consistent with differential measurements [9—11], might influence positively the thermal lattice calculations, avoiding unjustified increase of the average energy $\langle E \rangle$ of PFNS.

The phenomenological approach, developed in [14], was extended towards the emissive fission domain up to E_n = 20 MeV [1—6]. Analysis of the measured PFNS for neutron-induced fission of ^{232}Th, ^{235}U and ^{238}U shows that a number of data peculiarities could be correlated with the influence of (n, xnf) pre-fission neutron spectra on the observed prompt fission neutron spectra. For example, predicted partial contributions of the first-chance ^{235}U(*n, f*), second-chance ^{235}U(*n, nf*) and third-chance ^{235}U(*n, 2nf*) fission reactions to the observed fission cross section of ^{235}U(*n, F*) reaction allows reproduction of the measured PFNS average energy $\langle E \rangle$ variation over the incident neutron energy range of E_n= 5-20 MeV. Figures 2a, 2b show the comparison of $\langle E \rangle$ for ^{235}U(*n, F*) and ^{238}U(*n, F*). In case of ^{235}U(*n, F*) partial ^{235}U(*n, xnf*) contribution are fixed unambiguously [2], while ^{238}U(*n, xnf*) partial contributions are supported by the surrogate fission

data of ^{237}U(*n, f*) reaction cross section (see [17] and references therein). Pre-fission (*n, xnf*) neutron emission lowers the excitation energies of residual U nuclides. In case of ^{238}U(*n, F*) reaction the spectra of the pre-fission (*n, xnf*) neutrons appear to be rather soft, as compared with the spectra of neutrons, emitted by primary fission fragments after scission of the ^{238}U and ^{237}U nuclides. Combined effect of these peculiarities leads to the lowering of the average energy of the PFNS of ^{235}U(*n, F*) (^{238}U(*n, F*)) in the vicinity of ^{235}U(*n, nf*) (^{238}U(*n, nf*)) and ^{235}U(*n, 2nf*) (^{238}U(*n, 2nf*)) reaction thresholds, which is compatible with measured PFNS average energy $\langle E \rangle$. Figures 2a, 2b show that the present calculated energies of the prompt fission neutron spectra $\langle E \rangle$ closely reproduces the dips, observed by Ethvignot et al. [18, 19] around ^{235,238}U(*n, nf*) and ^{235,238}U(n, 2nf) reaction thresholds. In case of JEFF-3.1 [20] or ENDF/VI [21] or ENDF/B-VII.0 [12] only qualitative consistency with measured $\langle E \rangle$ data is demonstrated: it is out of phase with ^{235}U(*n, xnf*) and ^{238}U(*n, xnf*) channel openings as well. In previous calculations with Madland-Nix model [15] the variation of $\langle E \rangle$ with increase of E_n was oddly simulated by unjustified increase of the second chance fission contribution to the fission observables. However, that approach fails to describe the PFNS shapes at E_n= 5-20 MeV. Figures 3a, 3b show the com-

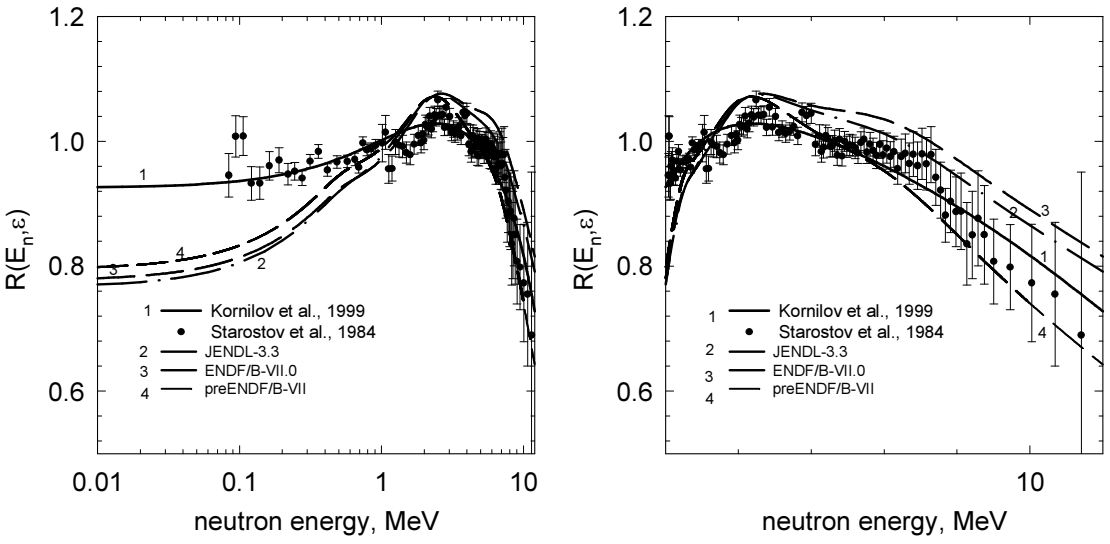

Figs. 1a, 1b. PFNS of ^{235}U(n, F) reaction at thermal energy relative to Maxwell average energy $\langle E \rangle$ =1.964 MeV.

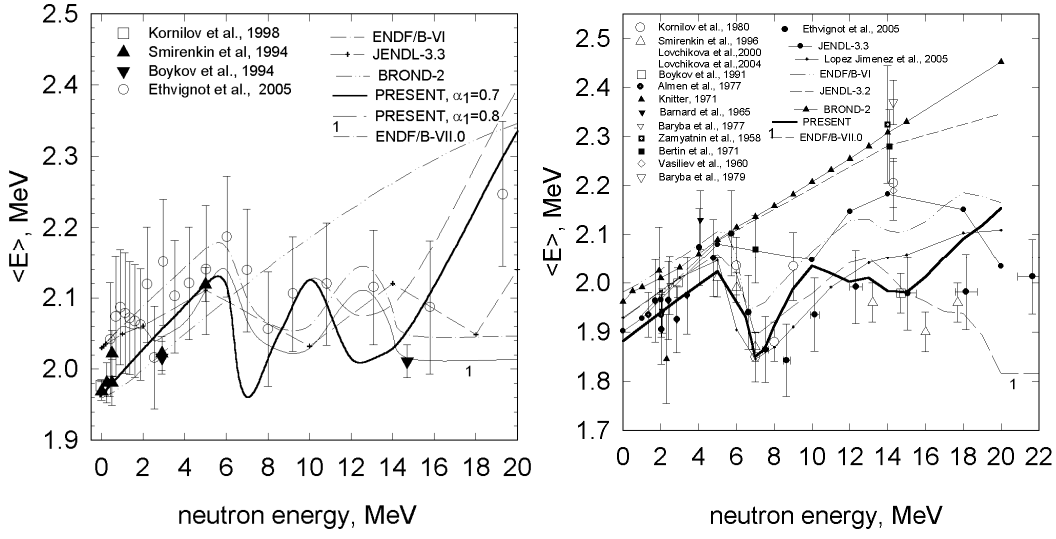

Figs. 2a, 2b. Average energy of the prompt fission neutron spectrum for ^{235}U(*n, F*) and ^{238}U(*n, F*).

parison of PFNS at E_n= 7 MeV for ^{235}U(*n, F*) (first observed by Frehaut et al. [22]) and ^{238}U(*n, F*) (first observed by Kornilov et al. [23]). The sharp increase of soft neutron yield at $\varepsilon < 1$ MeV is exemplified in case of both reactions. The shape of pre-fission neutron contribution much depends upon the fissility of target nuclide and relevant emissive fission contributions, being most pronounced in case of ^{232}Th(n, F) and least pronounced in case of ^{235}U(*n, F*) reaction. At higher incident neutron energy of 14.7 MeV, observed PFNS are composed of (*n, f*), (*n, nf*) and (*n, 2nf*) fission reaction contributions. The (*n, nf*) reaction contribution produces the broad spikes around 7 MeV, and strongly influence the soft part of PFNS (see Figs. 4a and 4b). Obviously, no other approach could reproduce the measured data as good as the present one.

Condensed representation of pre-fission neutron influence on PFNS of ^{239}Pu(*n, F*) is given on Fig. 5a. Predicted shape of the ^{239}Pu(*n, F*) $\langle E \rangle$ is much similar to that observed for ^{235}U(*n, F*) reaction [2, 19]. Though evaluations ENDF/B-VII.0 [12] (at E_n~ 15 MeV) and JEFF-3.1 [20] predict the variation of $\langle E \rangle$ above the $E_{n,nf}$ reaction threshold, they fail to attribute it to the precise variation of the relative contributions of pre-fission and prompt fission neutrons

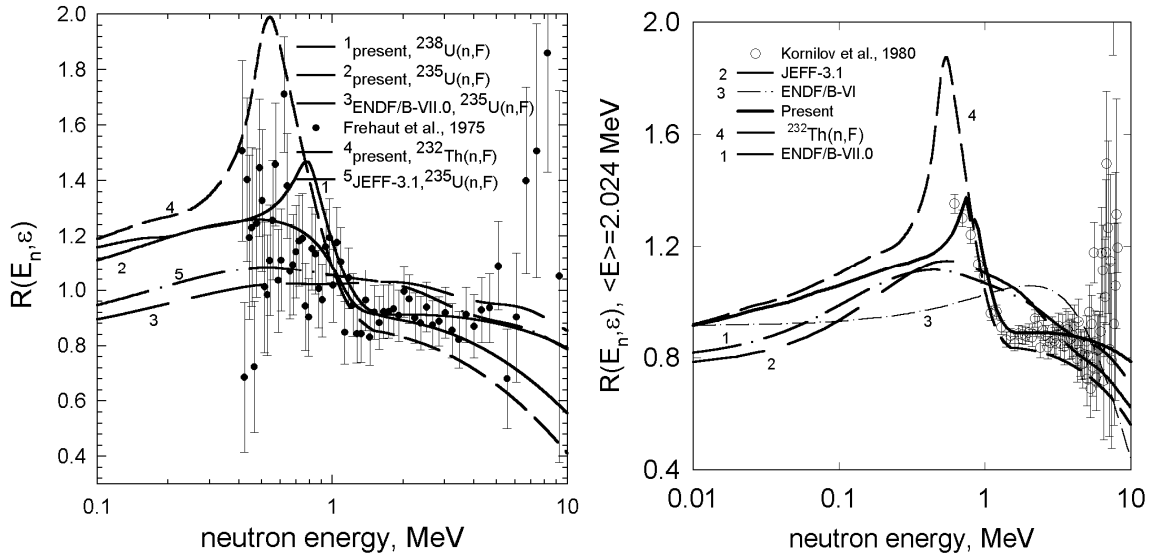

Figs. 3a, 3b. PFNS of ^{235}U(*n, F*) and ^{238}U(*n, F*) reactions at E_n = 7 MeV relative to Maxwell PFNS.

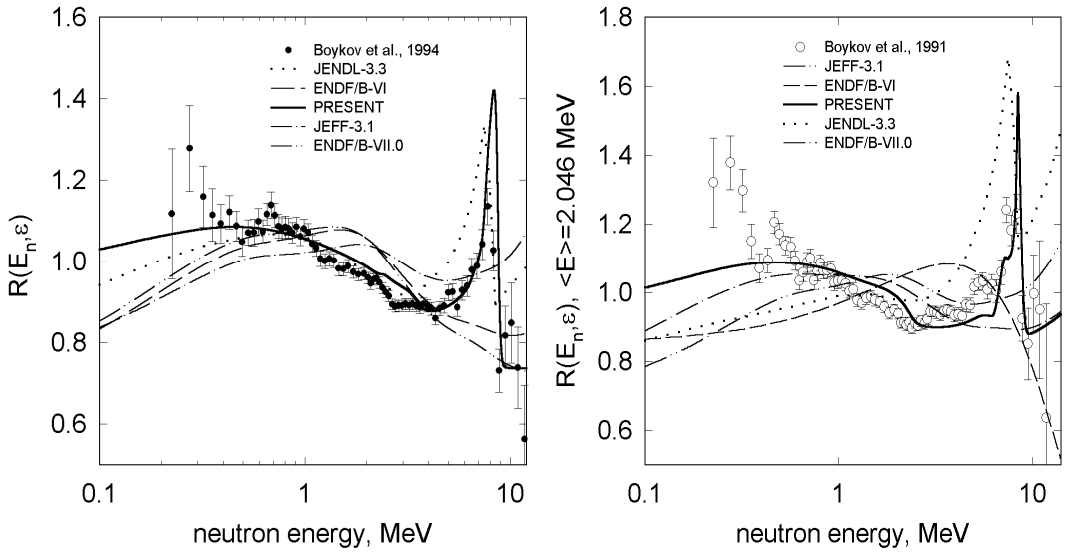

Figs. 4a, 4b. PFNS of ^{235}U(*n, F*) and ^{238}U(*n, F*) reactions at E_n = 4.7 MeV relative to Maxwell PFNS.

emitted by fission fragments. At $E_n > E_{n,nf}$ the lowering of $\langle E \rangle$, evident in present calculation, is missing in previous evaluations [12, 13] or shifted to higher energies [20]. The decrease of $\langle E \rangle$ of ENDF/B-VII.0 [12] at E_n~ 15 MeV is not supported by the measured data trend for ^{235}U(*n, F*) reaction [2, 19]. Present estimate of $\langle E \rangle$ is supported by the renormalized [24] value of $\langle E \rangle$ at E_n~ 1.5 MeV. It nicely reproduces PFNS shape of thermal neutron-induced fission of ^{239}Pu(*n, F*) [9]. Data by Knitter et al. [25] on $\langle E \rangle$ at $E_n \geq$ 2 MeV are scattering a lot and seem to be model-dependent. Data point by Zamyatnin et al. [26, 27] at E_n~ 14 MeV is based on rather narrow range of prompt fission neutrons. It might be argued that the dicrepancies of the measured and various evaluated data on $\langle E \rangle$ are well outside the nuclear application requests. That means the phenomenological/theoretical analysis of the actinide PFNS measured data, fixed at thermal energy point, helps to increase the reliability of the predictions for the ^{239}Pu(*n, F*) up to E_n~ 20 MeV.

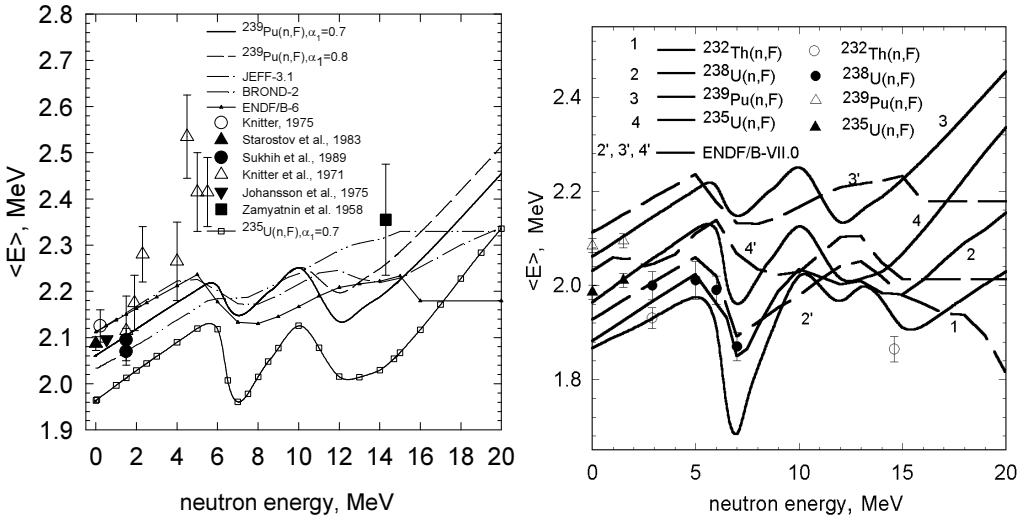

Figs. 5a, 5b. Average energy of PFNS for ^{232}Th(*n, F*) ^{235}U(*n, F*), ^{238}U(*n, F*) and ^{239}Pu(*n, F*).

Summarizing, we argue that correct estimates of the exclusive pre-fission (*n, xnf*) reaction spectra, alongside with simple modeling of spectra of neutrons, emitted from the fission fragments, allows a reproduction of the prompt fission neutron spectra for ^{232}Th(*n, F*), ^{235,238}U(*n, F*) and ^{239}Pu(*n, F*) reactions up to E_n = 20 MeV. Modeling of the spectra of neutrons, emitted from the fission fragments, appears to be rather crude, however it nicely reproduces measured PFNS for ^{232}Th(*n, F*) [1], ^{235}U(*n, F*) [2, 3], ^{238}U(*n, F*) [2, 4] and ^{239}Pu(*n, F*) [5, 6] reactions and might be used for PFNS prediction for the target nuclides with various fissilities, like ^{237}Np [28]. Figure 5b shows the comparison of $\langle E \rangle$ of PFNS for ^{232}Th, ^{238}U, ^{235}U and ^{239}Pu target nuclides, calculated with the present model, with data of ENDF/B-VII.0 [12] for ^{238}U, ^{235}U and ^{239}Pu. Measured data for ^{235}U(*n, F*) and ^{239}Pu(n, F) are shown for thermal neutrons and E_n= 1.5 MeV. For ^{239}Pu(*n, F*) there is no other reliable measured data. For ^{238}U(*n, F*) only data in the vicinity of the ^{238}U(*n, nf*) reaction threshold are shown, for ^{232}Th(*n, F*) all available data are shown. In our calculations there is a strict correlation of the "dips" in PFNS average energies with emissive fission contributions to the observed fission cross sections. Pre-fission neutrons influence is strongest in case of ^{232}Th(*n, F*) reaction and weakest in case of ^{239}Pu(*n, F*). That peculiarity is not due to the fact, that ^{239}Pu(*n, F*) fission fragments are most heated, but with the highest contribution of the first chance fission to the ^{239}Pu(*n, F*) fission cross section. In recent calculations by Madland [16], which are in fact used for the ENDF/B-VII.0 [12], this correlation is not pronounced. That is a convincing illustration of the importance of the precise description of the observed PFNS for the investigation of sharing of the excitation energy between the

fission fragments and pre-fission neutrons as well as prompt fission neutron spectra simulation.

The analysis of PFNS for ^{232}Th(*n, F*), ^{235}U(*n, F*), ^{238}U(*n, F*), ^{237}Np(*n, F*) and ^{239}Pu(*n, F*) reactions demonstrated, that a number of measured data peculiarities might be correlated (*n, xnf*) pre-fission neutron emission. The soft neutron contribution to the calculated PFNS is rather appreciable, as compared with neutrons, emitted by fission fragments. Recently the estimate of $\langle E \rangle$ for ^{239}Pu(*n, F*) was nicely confirmed by the experimental data by LANL (USA) and CEA (France) collaboration [7, 8], presented at this Consultants Meeting [29].

Present approach have been used for the evaluated data files compilation of ^{232}Th, ^{231}Pa, ^{233}Pa, ^{232}U, ^{234}U, ^{233}U, ^{238}U (http://www-nds.iaea.org/minskact), prepared with the ISTC support under the Project B-404. The validation of the ^{233}U evaluated data file has been performed against criticality safety benchmark experiments for high-enriched ^{233}U sphere with a fast spectrum. The Monte Carlo code calculations demonstrated a good agreement with experimental data. The prompt fission neutron spectra representation gave quite good description of K_{eff} [30].

The support of International Science and Technology Center (Moscow) under the Project Agreement B-1604) is acknowledged

REFERENCES

1. Maslov, V.M., Porodzinskij, Yu.V., Baba, M., et al., Prompt fission neutron spectra of ^{238}U and ^{232}Th above emissive fission threshold, Phys. Rev. **C69** (2004) 034607(1) — 34607(13).
2. Maslov,V.M., Kornilov, N.V., Kagalenko, A.B., et al., Prompt fission neutron spectra of ^{235}U above emissive fission threshold, Nucl. Phys. **A760** (2005) 274-302.
3. Maslov, V.M., ^{235m}U and ^{235}U neutron-induced fission, Abstracts of International Conference on Nuclear Data for Science and Technology, 22-27 April 2007, Nice, France, 2007, p.54.
4. Maslov, V.M., Prompt fission neutron spectra of ^{238}U. Phys. Atom. Nucl. **71** (2008) 9-26.
5. Maslov, V.M., Spectra of the prompt fission neutrons of the U and Pu fission higher than emissive fission neutrons. VANT, Ser. Reactor Physics. Moscow (2006) 33-40.
6. Maslov, V.M., ^{239}Pu prompt fission neutron spectra, Atomic Energy **103**, No. 2 (2007) 633-640.
7. Haight, R., Nuclear data research at Los Alamos Neutron Science Center, pp. 415-420 in Proc. Int. Conf. on Nuclear Data for Science and Technology (O. Bersillon, F. Gunsing, E. Bauge, R. Jacqmin and S. Leray, eds.), Nice, France, 22-27 April 2007, EDP Sciences, 2008.
8. Taieb, J., et al., Measurement of the average energy and multiplicity of prompt fission neutrons from ^{237}Np(n, F) from 0.7 to 200 MeV, pp. 429-432 in Proc. Int. Conf. on Nuclear Data for Science and Technology (O. Bersillon, F. Gunsing, E. Bauge, R. Jacqmin and S. Leray, eds.), Nice, France, 22-27 April 2007, EDP Sciences, 2008.
9. Starostov, B.I., Nefedov, V.N., Boycov, A.A., Prompt neutrons spectra from the thermal neutron fission of U-233, U-235, Pu-239 and spontaneous fission of Cf-252 in the secondary neutron energy range 0.01 - 12 MeV, Vop. At. Nauki i Tekhn., Ser.Yad. Konstanty **3** (1985) 16; EXFOR 40930;
   High precision prompt neutron spectra measurements for neutrons from Cf-252, U-233, U-235, Pu-239 fission in the energy range 2-11 MeV, pp. 290-293 in Proc. All Union Conf. on Neutron Physics, 2-6 October 1983, Kiev, Moscow, 1984. (in Russian); EXFOR 40872.

10. Wang Yufeng, Bai Xixiang, Li Anli, Wang Xiazhong, Li Jingwen, Meng Jiangchen, Bao Zongyu, An Experimental study of the prompt neutron spectrum of the ^{235}U fission induced by thermal neutrons, Chin. Jour. Nucl. Phys. **11**, No. 4 (1989) 47.
11. Lajtai, A., Kecskemeti, J., Safar, J., Dyachenko, P.P., Piksaikin, V.M., pp. 613-616 in Proc. Int. Conf. on Nuclear Data for Basic and Applied Sciences (P.G. Young, R. Brown, G.F. Auchampaugh, P.W. Lisowski, L. Stewart, eds.) Santa Fe, NM, USA, 13-17 May 1985, Vol. 1, Gordon and Breach, 1986.
12. Chadwick, M.B., Oblozinsky, P., Herman, M., et al., ENDF/B-VII.0: Next generation evaluated data library for nuclear science and technology, Nucl. Data Sheets **107** (2006) 2931-3060.
13. Shibata, K., Kawano, T., Nakagawa, T., et al., Japanese Evaluated Nuclear Data Library Version 3 Revision-3: JENDL-3.3, Nucl. Sci. Technol. **39** (2002) 1125-1199.
14. Kornilov, N.V., Kagalenko, A.B, Hambsch, F.-J., Calculation of the prompt fission neutron spectra on the basis of new systematic of the experimental data, Phys. At. Nucl. **62** (1999) 209—220.
15. Madland, D., Total prompt energy release in the neutron-induced fission of ^{235}U, ^{238}U and ^{239}Pu neutron spectra and average prompt neutron multiplicities, Nucl. Phys. **A772** (2006) 113—151.
16. Madland, D., Nix, J., New calculation of prompt fission neutron spectra and average prompt neutron multiplicities, Nucl. Sci. Eng. **81** (1982) 213—271.
17. Maslov, V.M., ^{237}U neutron-induced fission cross section, Phys. Rev. **C72** (2005) 044607.
18. Ethvignot, T., Devlin, M., Drosg, R., Granier, T., Haight, R.C., Morillon, B., Nelson, R.O., O'Donnel, J.M., Rochman, D., Prompt fission neutron average energy for ^{238}U(*n, F*) from threshold up to 200 MeV, Phys. Lett. **B575** (2003) 221-227.
19. Ethvignot, T., Devlin, M., Duarte, H., Granier, T., Haight, R.C., Morillon, B., Nelson, R.O., O'Donnell, J.M., Rochman, D., Neutron multiplicity in the fission of ^{238}U and ^{235}U with neutrons up to 200 MeV, Phys. Rev. Lett. **94** (2005) 052701.
20. Romain, P., Morillon, B., et al., JEFF-3.1, 2005 (available at http//:www.nea.fr).
21. Roussin, R.W., Young, P.G., McKnight, R., p. 692 in Proc. Int. Conf. Nuclear Data for Science and Technology, Gatlinburg, USA, 9-13 May 1994, J.K. Dickens (Ed.), American Nuclear Society, 1994.
22. Frehaut, J., Bertin, A., Bois, R., p 349 in Proc. Third All-Union Conf. on Neutron Physics, Kiev, 9-13 June, 1975, 1975, Vol. 5.
23. Kornilov, N.V., Zhuravlev, B.V., Salnikov, O.A., et al., pp. 44-49 in Proc. 5th Conf. on Neutron Physics, Kiev, 15-19 September 1980, Moscow, 1980, Vol. 2.
24. Lovchikova, G.N., Smirenkin, G.N., Trufanov, A.M., et al., Phys. Atom. Nucl. **62** (1999) 1551.
25. Knitter, H.H., Atomkernenergie **26** (1975) 76.
26. Zamyatnin, Yu.S., Safina, I.N., Gutnikova, E.K., et al., Atomnaya Energiya **4** (1958) 337.
27. Zamyatnin, Yu.S., Safina, I.N., Gutnikova, E.K., et al., Atomnaya Energiya **4** (1958) 443.
28. Maslov, V.M., Average energy of ^{237}Np and ^{241}Am prompt fission neutron spectra, Atom. Energy 104, No. 4 (2008) 330.
29. Bauge, E., this workshop.
30. Degtyarev, I.I., Maslov, V,M, "Criticality safety benchmark calculations using modern evaluated data libraries", pp. 865-868 in Proc. Inter. Conf. on Nuclear Data for Science and Technology (O. Bersillon, F. Gunsing, E. Bauge, R. Jacqmin and S. Leray, eds.), Nice, France, 22-27 April 2007, EDP Sciences, 2008.

Evaluation of Precise Fission Neutron Spectra for Actinides

M. Chadwick
Los Alamos National Laboratory, USA

Overview

- 4 Summary viewgraphs I presented at the IAEA/INDC meeting, on motivation for an international coordinated research effort on fission neutron spectra

- Aspects of fission neutron evaluations
  - Theory & Uncertainty Quantification
  - Experiments at LANL
  - Preequilibrium processes
  - (n,2n) dosimetry detectors - Bethe sphere testing & critical assemblies

NNSA — Los Alamos

Evaluation of Precise Fission Neutron Spectra for Actinides

Motivation:

- Accurate predictions of criticality are central to many applications - reactors and waste transmutation technologies, nonproliferation, *etc*
- Many labs have determined that current uncertainties in the fission spectrum ***represent one of the biggest sources of uncertainty in k-eff*** predictions (esp. recent work at LANL, Argonne/INL, Japan, Europe ...)
- A new collaboration could largely reduce the spectrum uncertainties.

Other background information:

- Dosimetry benchmark testing suggests ENDF/B-VII (Madland's work) high-energy spectrum too hard for 235U,239Pu in fast neutron energy region; too soft for thermal? (Mannhart) - **see later viewgraphs**
- ENDF community rejected Madland's newest 235U at thermal because of poor performance in thermal benchmarks. We need to resolve this.
- For 239Pu and 235,8U, few precise measurements exist below ~ 1 MeV emission energy, and above ~ 7 MeV emission energy. We presently rely on old models that are calibrated to the few measured data.

NNSA — Los Alamos

NIIAR Measurements of Fission Neutron Spectra: Summary based on Russian publications and EXFOR database

V.G. Pronyaev
6 November 2008

Following the development of methods to measure fission neutron spectra at the NIIAR, these measurements and publication of the results continued from the early 1970s to 1985. Many papers have been published at Kiev conferences and in Yadernye Konstanty, along with the results to be found in the EXFOR database. I am mainly considering the most recent Russian publication in Yadernye Konstanty, Vol. 3, p.16 (1985) by B.I. Starostov, V.N. Nefedov, A.A. Bojtsov, as representing a full review of the measurements of this group and their final results in the form of plots. Measurement details, corrections and uncertainties, final results to be found in different EXFOR entries are given below, along with what I considered to be errors in the EXFOR compilations.

1. Measurements

The time-of-flight method with flight paths varying between 10.4 and 611 cm was used to measure fission neutron spectra over a wide energy range from 0.01 to 12 MeV. "Zero" time was the moment at which fission fragments were detected to register nuclear fission; registration of fission neutrons with time delay after the fission event gave an estimation of the energy of the neutron. ^{252}Cf and ^{235}U targets were placed in ionization chambers. A chamber with ^{235}U target was installed along the flight path of the collimated thermal neutron beam filtered from fast neutrons and gammas by 12-cm thick layer of quartz and 8-cm layer of bismuth. Different forms of detector shielding were designed for the various flight paths in order to reduce the background of scattered neutrons. Efficiency of registration of the fission fragments was above 95% for ^{252}Cf and ^{235}U over all measurement cycles. Uncertainty in "zero" time for all measurements was 0.3 nsec. Neutron detectors were installed at an angle of 45 degrees to the plane of the target in order to neutralize the spectral distortion by the non-isotropy of registration for the fission fragments.

Two measurement cycles were carried out:

Cycle No. 1 was undertaken with a miniature ionization chamber (MIC, 2.5 g) to register fission fragments, along with different flight paths and scintillation detectors. Three different series of measurements were conducted:
1.1. Flight path of 51-cm; anthracene detector; energy interval for measurements of 0.1 to 2 MeV (uncertainty in the efficiency of 2.5%).
1.2. Flight path of 231.3 cm; stilbene detector; energy interval for measurements of 1.4 to 8 MeV (uncertainty in the efficiency = uncertainty of the standard).
1.3. Flight path of 611-cm; plastic detector; interval for measurements of 3 to 12 MeV (uncertainty in the efficiency = uncertainty of the standard).

Cycle No. 2 involved gaseous scintillation detectors (GSD) for fission fragment registration, different flight paths, and two types of non-threshold neutron detector (i.e. two different sets of measurements):
2.1. Flight paths of 12.4, 21.4 and 40 cm; non-threshold ionization chambers (IC) with eight layers of ^{235}U; energy interval for measurements of 0.01 to 5 MeV (uncertainty in the efficiency less than 4%); and used only for measurements of ^{252}Cf fission neutron spectra.

2.2. Flight path of 10.4, 21.4 and 29.5 cm; gaseous scintillation detector-ionization chamber (GSDIC) with metallic ^{235}U radiator; energy interval for measurements of 0.01 to 5 MeV (uncertainty in the efficiency is determined by the uncertainty in the ^{235}U fission cross section).

Counting rates are lowest for **1.3** flight path, with 8000 counts for neutrons of energy 4 MeV, and 70 counts for neutrons with an energy of 14 MeV for 240 hours of continuous measurements.

2. Data processing

All determinations of data and their uncertainties, related to the distances, angles, numbers of counted neutrons and fission events, time channel width, and position of "zero" time, were obtained by methods described in: L.M. Green *et al*., Nucl. Sci. Eng. **50**(3) p.257 (1973); B.I. Starostov *et al*., NIIAR preprint П-12 (346) (1978)).

The effect of anisotropy on the registration of the fission fragments was studied experimentally, and was found to be negligible.

Time-of-flight spectra were transformed into energy spectra after background correction. Further corrections were introduced into these energy spectra: background neutrons scattered by the target backing, gas atoms, walls of the MIC and GSD, the air within Ω angle, the lead shielding of the detectors from the delayed-gamma and all structural parts of the neutron detector. After these corrections, the intensity ratio ^{252}Cf / ^{235}U for energy spectra in the energy interval from 0.01 to 12 MeV was obtained. This ratio is independent of the systematic uncertainties in the determination of the efficiency of the neutron detector.

Detector efficiency for **cycle No. 1** measurements was calculated for the anthracene detector by means of the Monte Carlo method, and taking into account single and double scattering of neutrons on hydrogen, nonlinearity of the photon yield for the scintillator, neutrons and gammas in the ^{12}C(n,n') and ^{12}C(n,n'γ) reactions, and neutrons scattered in the photo-electrical multiplier with time shift corrections. The method used to choose the threshold for neutron registration of the different detectors does not lead to discrepancies between data in the energy regions where they overlap. A calculated detector efficiency for the absolute normalization of the spectra was only used for the anthracene detectors - calculated uncertainties for the anthracene detector efficiency were below 2.5%. The efficiencies of the stilbene and plastic-scintillator detectors were determined on the supposition that the shape of the ^{252}Cf(sf) fission neutron spectrum is known. Such "known" spectrum was obtained by averaging (via evaluation) the data measured by many authors (see Table 2 of the paper - results are given below as taken from EXFOR in Attachment 1) - these data were used to calculate the stilbene and plastic-scintillator detector efficiencies. Efficiencies of the detectors were consistent (within 3%) with the efficiencies calculated using the Monte Carlo technique.

IC and GSDIC detector efficiencies for the **cycle No. 2** measurements of ^{252}Cf were judged to be proportional to the ^{235}U(n,f) cross section evaluated by V. Kon'shin and co-workers in 1978. I assume that this evaluation was inserted into the BROND-2 library for ^{235}U. Comparison of these data with ENDF/B-VII are shown at Fig. 1 of Attachment 2, and do not show any large differences in shape above a neutron energy of 15 keV. ^{235}U(n,f) data from BROND-2 are also given. Difficulties were experienced in the ^{235}U(n_{th},f) measurements with respect to background corrections (*closed geometry and large corrections? - VP*), and measurements were undertaken relative to ^{252}Cf(sf), with the fission neutron spectrum adopted as given in Appendix 1.

Finally, correction for the spectral resolution, suggesting that the shape of the spectra should be near-Maxwellian, was below 1.5%.

3. Uncertainties

Twenty partial components of the total uncertainty were considered. Some are uncertainties in the energy determination - those related directly to the cross-section determination are as follows:

- uncertainty in the neutron detector efficiency which is the largest partial (systematic) uncertainty
- uncertainty due to discrimination level stability
- uncertainty due to delayed gammas
- statistical uncertainty
- uncertainty due to random coincidence in the detector, which is also statistical in nature and is combined with the statistical uncertainty
- uncertainty due to "recycling" neutrons, which is also statistical in nature and is combined with statistical uncertainty
- uncertainty due to the experimental hall background, which has also statistical nature and is combined with statistical error
- uncertainty due to the flight time uncertainty
- uncertainty due to scattered neutrons.

4. Authors' conclusion

The results of the No. 1 and 2 cycles of measurements are consistent in the neutron energy range from 0.1 to 5 MeV.

Over the energy range of emitted neutrons from 0.01 to 7.5 MeV, the measured spectral shape deviates from Maxwellian by not more than 5% to 7%.

At energies above 7 MeV, there are large deviations from Maxwellian spectra.

V.G. Pronyaev: the following is my understanding (or misunderstanding) of the results from the point of view of the "primarily measured quantities" and the means of transforming to the quantities given by the authors:

1.1. series of measurements for ^{252}Cf(sf) and ^{235}U(n_{th},f) are absolute measurements. Data should be given as the number of neutrons per MeV.
1.2. series of measurements for ^{252}Cf(sf) and ^{235}U(n_{th},f) with the detector efficiency determined by means of the averaged spectrum of ^{252}Cf(sf). ^{252}Cf(sf) results for this series of measurements give only differences relative to this averaged spectrum, and ^{235}U(n_{th},f) results should exhibit the ratio to this averaged ^{252}Cf(sf) spectrum. Shape data (non-normalized) are given, and should be defined as ARB-UNITS (arbitrary). The ^{252}Cf(sf)/ ^{235}U(n_{th},f) ratio is only the directly measured quantity which does not depend from the detector efficiency determination.
1.3. series - same conclusion as for **1.2**.
2.1. series for ^{252}Cf(sf) measurements presents the results as only shape data (non-normalized) for the ratio of ^{252}Cf(sf) spectra to the ^{235}U(n,f) cross section (used as a standard for shape). Using the Kon'shin evaluation for the fission cross section, these data can be converted to shape data (non-normalized) for ^{252}Cf(sf) spectra. Data should be given as ARB-UNITS.
2.2. series - same conclusions for ^{235}U(n_{th},f) and ^{252}Cf(sf) as in the **2.1 series** for ^{252}Cf.

Table 1. Source of the latest results in EXFOR - data in EXFOR (approved by the authors in 1985-1986) compared with data at plots of final publication (YK, 3, p.16 (1985)).

Cycle Series	Reaction	EXFOR Subentry	Comment
1.1.	^{252}Cf(sf)	40874002	Data in EXFOR approved by authors, and presented as ratio to Maxwellian with kT = 1.42 MeV
	^{235}U(n_{th},f)	40871008	Data in EXFOR approved by authors in 06/1985. Since they are absolute measurements, data are given in this sub-entry as absolute spectra expressed in terms of the number of neutrons per MeV - but have been assigned incorrect ARB-UNITS in EXFOR
		40871007	Data in EXFOR approved by authors in 06/1985. Somehow normalized at a yield of 2.383 neutrons per fission, and should be given in this sub-entry as absolute spectra expressed in terms of the number of neutrons per MeV - but have been assigned incorrect ARB-UNITS in EXFOR. They are primarily obtained as shape-type data (ARB-UNITS) with efficiency of the detector evaluated using averaged ^{252}Cf(sf) fission neutron spectra
	^{252}Cf(sf)/^{235}U(n_{th},f)	40871011	Primarily measured absolute ratio, free from detector efficiency determination problems
1.2.	^{252}Cf(sf)	40871005	Data in EXFOR approved by authors in 06/1985 Somehow normalized at a yield of 3.77 neutrons per fission, and should be given in this sub-entry as absolute spectra expressed in terms of the number of neutrons per MeV - but have been assigned incorrect ARB-UNITS in EXFOR. They are primarily obtained as shape-type data (ARB-UNITS) with efficiency of the detector evaluated using averaged ^{252}Cf(sf) fission neutron spectra.
	^{235}U(n_{th},f)	40871007	Data in EXFOR approved by authors in 06/1985 Somehow normalized at a yield of 2.383 neutrons per fission, and should be given in this sub-entry as absolute spectra expressed in terms of the number of neutrons per MeV - but have been assigned incorrect ARB-UNITS in EXFOR. They are primarily obtained as shape-type data (ARB-UNITS) with efficiency of the detector evaluated using averaged ^{252}Cf(sf) fission neutron spectra
	^{252}Cf(sf)/^{235}U(n_{th},f)	40871012	Primarily measured absolute ratio, free from detector efficiency determination problems
1.3.	^{252}Cf(sf)	40872002	Data in EXFOR approved by authors in 06/1985 Somehow normalized at a yield of 3.77 neutrons per fission, and should be given in this sub-entry as absolute spectra expressed in terms of the number of neutrons per MeV - but have been assigned incorrect ARB-UNITS in EXFOR. They are primarily obtained as shape-type data (ARB-UNITS) with efficiency of the detector evaluated

			using averaged ^{252}Cf(sf) fission neutron spectra
	^{235}U(n_{th},f)	40872004	Data in EXFOR approved by authors in 06/1985 Somehow normalized at a yield of 2.383 neutrons per fission, and should be given in this sub-entry as absolute spectra expressed in terms of the number of neutrons per MeV - but have been assigned incorrect ARB-UNITS in EXFOR. They are primarily obtained as shape-type data (ARB-UNITS) with efficiency of the detector evaluated using averaged ^{252}Cf(sf) fission neutron spectra
	^{252}Cf(sf)/^{235}U(n_{th},f)	40872007	Primarily measured absolute ratio, free from detector efficiency determination problems
2.1.	^{252}Cf(sf)	40874003	Data in EXFOR approved by authors Data obtained with IC, and presented as ratio to Maxwellian with kT = 1.42 MeV ^{235}U(n,f) cross section is the standard for the shape of the ^{252}Cf(sf) spectra
	^{235}U(n_{th},f)	-	Small IC was only used for measurements of ^{252}Cf(sf) fission neutron spectra
2.2.	^{252}Cf(sf)	40874004	Data in EXFOR approved by authors Data obtained with GSDIC, and presented as ratio to Maxwellian with kT = 1.42 MeV ^{235}U(n,f) cross section is the standard for the shape of the ^{252}Cf(sf) spectra
	^{235}U(n_{th},f)	40873004	Data in EXFOR approved by authors Data are presented as ratio to Maxwellian with kT = 1.313 MeV Shape-type data, with the efficiency of the detector evaluated using averaged ^{252}Cf(sf) fission neutron spectra

Finally, the following data sets can be included in the least-squares fit and evaluation:

40874002 are the result of absolute measurements (but could be used as shape-type data) - neutron detector correlation with 40871008.

40871008 are the result of absolute measurements (but could be used as shape-type data) - neutron detector correlation with 40871002.

40871011 are the result of direct measurement of the normalized ratio (but could be used as shape-type data for ratio). If 40871011 is used, 40874002 and 40871008 should not be used (to avoid duplication and redundancy).

40871012 (with two data sets) are the result of direct measurement of normalized ratio (but could be used as shape-type data for ratio).

40872007 (with two datasets) are the result of direct measurement of normalized ratio (but could be used as shape-type data for ratio).

40874003 is measurement relative to the ^{235}U(n,f) cross section. Can be renormalized to the new ^{235}U(n,f) cross-section standard. Possess a common standard, and therefore have correlations with 40874004 and 40873004.

40874004 is measurement relative to the ^{235}U(n,f) cross section. Can be renormalized to the new ^{235}U(n,f) cross-section standard. Possess a common standard, and therefore have correlations with 40874003 and 40873004.

If more stringent conditions are adopted for selection, as proposed by Nikolai Kornilov (direct measurements and more accurate ratios for ^{235}U to ^{252}Cf spectra), only EXFOR sub-entries 40871011, 40871012 and 40872007 are appropriate for consideration as data for standard and reference spectra fit.

Table 2. Other data in the EXFOR database (data presented – most of my guesses are based on information given by the compiler).

EXFOR Sub-entry	Data presented
40871007	Data derived by combining the results of **1.1**. and **1.2. series** of measurements (given as a single data set, without the inclusion of overlapping data), and presented as absolute data (number of neutrons/MeV) There is no description of the procedure in REFERENCE – they were probably sent by authors to the compiling centre as additional data for compilation
40644002	Data derived by combining the results of all series of measurements (as a single dataset, without the inclusion of overlapping data), and presented as absolute data in the energy range from 14.3 keV to 10.14 MeV (number of neutrons per MeV) There is no explanation of how the data were combined

Table 3. Errors and misprints found in the current EXFOR database.

EXFOR Sub-entry	Important problem
40873001	MONITOR is the spectrum given in Table 4 of YK, vol. 3, p.20 (1985) (see also Attachment 1 or X4 = 40930002), which is presented as the ratio to the Maxwellian spectra with kT = 1.42 MeV, and not Maxwellian spectra with kT = 1.418
40871008	REACTION: not relative to the Maxwellian
40871005	REACTION: should be (sf) and not (n,f) Data units are probably the number of neutrons per MeV
40871007	Data units should be the number of neutrons per MeV
40871008	Data units should be the number of neutrons per MeV
40872001	DETECTOR (SCIN) free text should be “plastic scintillator for neutron spectrum measurements”
40872002	Data are given as number of neutrons per MeV, although they are shape-type data
40872004	Data are given as number of neutrons per MeV, although they are shape-type data
40873001	MONITOR is the spectrum given in Table 4 of YK, vol. 3, p.20 (1985) (see also Attachment 1 or X4 = 40930002), which is presented as the ratio to the Maxwellian spectra with kT = 1.42 MeV, and not Maxwellian spectra with kT = 1.418
40873004	REACTION: should be relative Maxwellian with kT = 1.313 MeV
40874002	Data units should be the number of neutrons per MeV – absolute measurements
40874001	DETECTOR: (SCIN) anthracene detector for neutron registration should be moved to 40874002
40874003	DETECTOR should be “(IOCH) thin-wall ionization chamber with eight ^{235}U fission layer for neutron registration”
40874003	DETECTOR should be “(IOCH) gas scintillating detector - ionization chamber with ^{235}U metallic radiator”
40930002	Data are the result of much experimental data averaging used to determine the efficiency of the detectors - they should be inserted (as evaluated data - monitor) in all subentries of **cycles 1.2. and 1.3**

Attachment 1. ^{252}Cf(sf) fission neutron spectra used to determine the absolute efficiency of the stilbene (case 1.2. for cycle 1) and plastic detectors (case 1.3. for cycle 1) given as ratio to the Maxwellian spectrum with kT = 1.42 MeV.

```
SUBENT        40930002   19990311   19990705   20050926       000040930002    1
BIB                 4         12                                 40930002    2
REACTION   ((98-CF-252(0,F),PR,DE,N,,EXP)//                      40930002    3
           (98-CF-252(0,F),PR,DE,N,,CALC))  RELATIVE TO THE      40930002    4
               MAXWELL SPECTRUM WITH TEMPERATURE 1.42 MEV         40930002    5
STATUS     (TABLE)  DATA ARE TAKEN FROM TABLE 4 OF MAIN REFERENCE 40930002    6
           (COREL,40874003)  DATA IN THIS SUBENT COVER THE WHOLE  40930002    7
           (COREL,40874004)  ENERGY RANGE IN DIFFERENCE TO SUBENT 40930002    8
                             40874002 AND 40874004                40930002    9
FLAG       (1.)  INDEPENDENT VARIABLE CHANGED BY COMPILER         40930002   10
HISTORY    (19990311A)  REACTION VALUE IS GIVEN EXPLICITELY AS    40930002   11
                        RATIO OF TWO VALUES                       40930002   12
           (19990405A)  NEW REACTION-QUANTITY RATIOS CODING GIVEN 40930002   13
                        E-NM AND E-DN INTRODUCED                  40930002   14
ENDBIB             12                                             40930002   15
COMMON              1          3                                   40930002   16
E-DN                                                              40930002   17
MEV                                                               40930002   18
  1.42                                                            40930002   19
ENDCOMMON           3                                             40930002   20
DATA                5        110                                  40930002   21
E-NM       E-RSL      DATA       ERR-T      FLAG                  40930002   22
MEV        MEV        NO-DIM     PER-CENT   NO-DIM                40930002   23
  3.000E-04  1.0  E-04  1.084E-00  40.                            40930002   24
  7.000E-04  2.0  E-04  1.084E-00  30.                            40930002   25
  1.500E-03  4.0  E-04  9.58 E-01  20.                            40930002   26
  2.500E-03  3.0  E-04  9.58 E-01  15.                            40930002   27
  3.400E-03  3.0  E-04  9.72 E-01  10.                            40930002   28
  4.4  E-03  3.0  E-04  9.72 E-01  10.                            40930002   29
  5.5  E-03  3.0  E-04  9.57 E-01   9.                            40930002   30
  6.5  E-03  3.0  E-04  9.55 E-01   8.                            40930002   31
  7.5  E-03  3.0  E-04  9.83 E-01   8.                            40930002   32
  8.4  E-03  4.0  E-04  9.83 E-01   8.                            40930002   33
  9.5  E-03  6.0  E-04  9.75 E-01   7.                            40930002   34
  1.540E-02  2.6  E-03  9.73 E-01   7.                            40930002   35
  3.440E-02  2.1  E-03  9.65 E-01   7.                            40930002   36
  6.000E-02  2.00 E-03  9.71 E-01   6.                            40930002   37
  8.100E-02  3.0  E-03  9.88 E-01   5.                            40930002   38
  9.100E-02  3.0  E-03  1.000E-00   4.                            40930002   39
  1.040E-01  3.0  E-03  1.028E-00   3.                            40930002   40
  1.150E-01  3.0  E-03  1.026E-00   3.                            40930002   41
  1.340E-01  3.0  E-03  1.010E-00   2.5                           40930002   42
  1.440E-01  3.0  E-03  1.018E-00   2.5                           40930002   43
  1.550E-01  3.0  E-03  9.99 E-01   2.5                           40930002   44
  1.660E-01  3.0  E-03  9.83 E-00   2.5                           40930002   45
  1.780E-01  3.0  E-03  9.70 E-01   2.5                           40930002   46
  1.940E-01  4.0  E-03  9.62 E-01   2.5                           40930002   47
  2.070E-01  4.0  E-03  9.64 E-01   2.5                           40930002   48
  2.210E-01  4.0  E-03  9.68 E-01   2.5                           40930002   49
  2.390E-01  5.0  E-03  9.75 E-01   3.                            40930002   50
  2.630E-01  6.0  E-03  9.74 E-01   3.                            40930002   51
  2.87 E-01  6.0  E-03  9.89 E-01   3.                            40930002   52
  3.20 E-01  6.0  E-03  9.82 E-01   3.                            40930002   53
  3.30 E-01  7.0  E-03  9.89 E-01   3.        1.                  40930002   54
  3.57 E-01  8.0  E-03  9.88 E-01   2.                            40930002   55
  3.82 E-01  8.0  E-03  9.82 E-01   2.                            40930002   56
  4.27 E-01  8.0  E-03  9.89 E-01   2.                            40930002   57
  4.56 E-01  8.0  E-03  9.73 E-01   2.                            40930002   58
  4.99 E-01  8.0  E-03  9.76 E-01   2.                            40930002   59
  5.49 E-01  8.0  E-03  9.79 E-01   2.                            40930002   60
  6.31 E-01  6.0  E-03  9.62 E-01   2.                            40930002   61
  6.92 E-01  6.0  E-03  9.76 E-01   2.                            40930002   62
  7.37 E-01  6.0  E-03  9.77 E-01   2.                            40930002   63
  8.03 E-01  7.0  E-03  9.73 E-01   2.                            40930002   64
  8.68 E-01  9.0  E-03  9.78 E-01   2.                            40930002   65
  9.06 E-01  1.1  E-02  1.000E-00   2.                            40930002   66
  1.002E-00  2.8  E-02  9.96 E-01   2.                            40930002   67
  1.050E-00  2.8  E-02  1.002E-01   2.                            40930002   68
  1.170E-00  2.8  E-02  1.011E-01   2.                            40930002   69
  1.260E-00  2.9  E-02  1.023E-01   3.                            40930002   70
  1.353E-00  3.5  E-02  1.028E-01   2.5                           40930002   71
  1.480E-00  2.9  E-02  1.044E-01   2.5                           40930002   72
  1.640E-00  2.6  E-02  1.026E-01   2.5                           40930002   73
  1.760E-00  2.5  E-02  1.020E-01   2.5                           40930002   74
```

1.836E-00	2.6	E-02	1.027E-01	2.	40930002	75
1.990E-00	3.0	E-02	1.024E-01	2.	40930002	76
2.123E-00	3.1	E-02	1.023E-01	2.	40930002	77
2.216E-00	3.1	E-02	1.027E-01	1.5	40930002	78
2.314E-00	3.1	E-02	1.024E-01	1.5	40930002	79
2.400E-00	3.1	E-02	1.030E-01	1.5	40930002	80
2.537E-00	3.8	E-02	1.034E-01	2.	40930002	81
2.662E-00	3.3	E-02	1.030E-01	2.2	40930002	82
2.772E-00	3.0	E-02	1.034E-01	2.5	40930002	83
2.875E-00	4.1	E-02	1.026E-01	2.6	40930002	84
2.964E-00	3.1	E-02	1.034E-01	2.2	40930002	85
3.151E-00	3.4	E-02	1.020E-01	2.	40930002	86
3.305E-00	3.3	E-02	1.024E-01	2.5	40930002	87
3.408E-00	6.2	E-02	1.015E-01	2.3	40930002	88
3.537E-00	6.2	E-02	1.015E-01	2.3	40930002	89
3.629E-00	6.8	E-02	1.014E-01	2.3	40930002	90
3.748E-00	6.8	E-02	1.014E-01	2.3	40930002	91
3.938E-00	6.2	E-02	1.017E-01	2.3	40930002	92
4.155E-00	6.2	E-02	1.015E-01	2.5	40930002	93
4.268E-00	6.2	E-02	1.015E-01	2.5	40930002	94
4.398E-00	6.5	E-02	1.017E-01	2.3	40930002	95
4.582E-00	6.5	E-02	1.015E-01	2.5	40930002	96
4.777E-00	6.5	E-02	1.015E-01	2.	40930002	97
4.986E-00	6.5	E-02	1.013E-01	2.	40930002	98
5.208E-00	6.5	E-02	1.018E-01	2.	40930002	99
5.446E-00	6.5	E-02	1.011E-01	3.	40930002	100
5.700E-00	6.5	E-02	9.99 E-01	4.	40930002	101
5.973E-00	6.5	E-02	9.93 E-01	4.	40930002	102
6.170E-00	1.5	E-01	9.89 E-01	4.	40930002	103
6.270E-00	1.5	E-01	9.88 E-01	4.	40930002	104
6.370E-00	1.6	E-01	9.88 E-01	4.	40930002	105
6.470E-00	1.6	E-01	9.89 E-01	4.	40930002	106
6.580E-00	1.6	E-01	9.87 E-01	4.	40930002	107
6.69	1.6	E-01	9.85 E-01	4.	40930002	108
6.81	1.6	E-01	9.89 E-01	5.	40930002	109
6.92	1.6	E-01	9.86 E-01	5.	40930002	110
7.04	1.6	E-01	9.86 E-01	5.	40930002	111
7.16	1.6	E-01	9.84 E-01	5.	40930002	112
7.29	1.6	E-01	9.80 E-01	5.	40930002	113
7.42	2.0	E-01	9.74 E-01	5.	40930002	114
7.55	2.0	E-01	8.69 E-01	5.	40930002	115
7.68	2.0	E-01	9.59 E-01	5.	40930002	116
7.82	2.0	E-01	9.52 E-01	5.	40930002	117
7.97	2.0	E-01	9.50 E-01	5.5	40930002	118
8.11	2.0	E-01	9.49 E-01	5.5	40930002	119
8.27	2.0	E-01	9.46 E-01	6.	40930002	120
8.42	2.0	E-01	9.43 E-01	6.	40930002	121
8.58	2.0	E-01	9.41 E-01	6.	40930002	122
8.75	2.0	E-01	9.32 E-01	6.	40930002	123
9.09	2.0	E-01	9.23 E-01	6.	40930002	124
9.46	2.0	E-01	9.15 E-01	6.5	40930002	125
9.92	2.0	E-01	9.27 E-01	6.	40930002	126
10.0	2.0	E-01	9.06 E-01	6.5	40930002	127
10.7	2.0	E-01	8.73 E-01	7.	40930002	128
11.3	2.0	E-01	8.50 E-01	7.	40930002	129
11.9	2.0	E-01	8.38 E-01	7.	40930002	130
12.5	2.0	E-01	8.31 E-01	8.	40930002	131
13.6	2.	E-01	7.89 E-01	9.	40930002	132
15.4	3.	E-01	7.72 E-01	10.	40930002	133

Attachment 2. ^{235}U fission cross sections used to calculate the energy dependence of the detector efficiency in cycle No. 2 measurements.

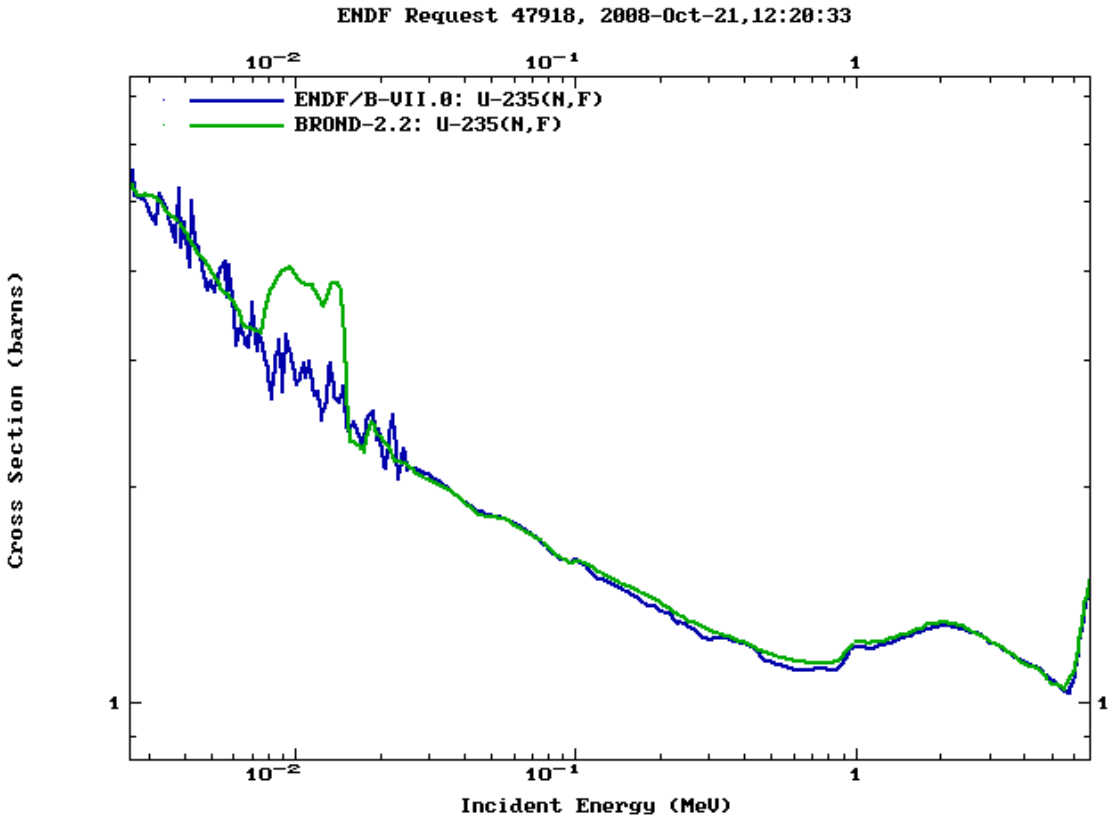

Fig. 1. Comparison of Kon'shin evaluation (1978) with ENDF/B-VII.0.

Table 1. Cross sections of ^{235}U(n,f) used to evaluate the energy dependence of the efficiency of the detectors in cycle 2 measurements.

# Energy	Cross section
# MeV	barns
0.0100437	3.94808
0.0103271	3.88585
0.0105	3.84787
0.0107963	3.84031
0.0111009	3.83253
0.0114141	3.82454
0.0115	3.82235
0.0118245	3.74199
0.012	3.69853
0.0123386	3.62146
0.0125	3.58472
0.0128527	3.68319
0.013	3.72432
0.0133668	3.81562
0.0135	3.84878
0.013625	3.85819
0.0136875	3.86029
0.01375	3.86085
0.013875	3.85771
0.014	3.84941
0.014125	3.83633
0.01425	3.81864
0.0143125	3.80806
0.0145	3.76912
0.01475	3.43044
0.014875	3.25625

0.015	3.07821
0.015125	2.89572
0.01525	2.70809
0.015375	2.51446
0.0155	2.31375
0.0159374	2.31238
0.016	2.31219
0.0164515	2.29604
0.0165	2.2943
0.0169656	2.27187
0.017	2.27021
0.0174797	2.24546
0.0175	2.24441
0.017625	2.28273
0.01775	2.31678
0.017875	2.34742
0.018	2.37527
0.01825	2.42437
0.0185	2.46671
0.01875	2.45287
0.019	2.43264
0.019125	2.42042
0.01925	2.40687
0.0195	2.37595
0.0200502	2.35068
0.02025	2.3415
0.020625	2.32138
0.021	2.29889
0.021375	2.27358
0.02175	2.24483
0.022125	2.21181
0.0225	2.17334
0.023125	2.1719
0.02375	2.16595
0.024375	2.15661
0.025	2.14467
0.0257054	2.12799
0.02625	2.11511
0.0269907	2.09447
0.0275	2.08028
0.028276	2.06855
0.0290738	2.0565
0.029375	2.05195
0.0302039	2.0412
0.0310561	2.03014
0.03125	2.02762
0.0321318	2.01843
0.0330384	2.00897
0.0339706	1.99925
0.0349292	1.98925
0.035	1.98851
0.0359876	1.97198
0.037003	1.95497
0.0380471	1.93749
0.0391207	1.91952
0.04	1.90479
0.0411287	1.88854
0.0422892	1.87184
0.0434824	1.85466
0.0447093	1.837
0.045	1.83281
0.0462697	1.8283
0.0475	1.82394
0.0488403	1.82071
0.05	1.81792

0.0514108	1.81638
0.0528615	1.8148
0.054353	1.81317
0.055	1.81246
0.0565519	1.80014
0.0581476	1.78747
0.0597883	1.77444
0.06	1.77276
0.061693	1.76098
0.0634338	1.74888
0.065	1.73798
0.0668341	1.72844
0.0687199	1.71862
0.07	1.71195
0.0719752	1.70289
0.074006	1.69356
0.075	1.689
0.0771162	1.67077
0.0792922	1.65202
0.08	1.64592
0.0822573	1.62774
0.0845783	1.60905
0.085	1.60566
0.0873984	1.59751
0.0898645	1.58913
0.0924001	1.58051
0.095	1.57168
0.1	1.57775
0.1	1.58098
0.126764	1.50533
0.152116	1.45355
0.223104	1.33876
0.25	1.302
0.29	1.267
0.443157	1.1877
0.47298	1.17578
0.514108	1.1639
0.608465	1.14432
0.709876	1.137
0.74503	1.137
0.8	1.139
0.85	1.147
0.9	1.168
0.95	1.202
1	1.22
1.1	1.215
1.23386	1.22322
1.45981	1.24633
1.8	1.288
2	1.298
2.23104	1.28983
2.46772	1.27157
2.98012	1.22109
3.90722	1.13942
4	1.132
4.5	1.111
5	1.064
5.5	1.047
6	1.11201
6.5	1.364
7	1.553
7.5	1.719
8	1.782
8.47892	1.782
10.0437	1.74895

10.6481	1.73622
11.1552	1.732
11.4052	1.732
11.5	1.732
12	1.748
12.5	1.826
13.1834	1.94545
13.5	1.998
14	2.068
14.5	2.099
15	2.103
16	2.068
17	1.986
18	1.939
19	1.966
20	2.045

Ratio of prompt fission neutron spectra from ^{252}Cf(sf) and ^{235}U(n_{th},f) reactions

V.G. Pronyaev (pronyaev@ippe.ru)

10 December 2008

As stated by Starostov *et al.*, their measurements of ratios of prompt fission neutron spectra for ^{252}Cf(sf) to ^{235}U(n_{th},f) reaction is most direct experimental result free for many problems related to the normalization. These ratio data were not included in the evaluation of prompt fission neutron spectra (used as standard and reference). Because they cover a wide energy range of secondary neutrons there is interest in comparing them with ratio of standards and reference spectra. The comparison is shown in Fig. 1 (in lin-log) and 2 (log-lin) presentations. Results of three sets of measurements shown by crosses of different colors are taken from EXFOR subentries. The authors obtained the absolute ratio of two fission neutron spectra, but for comparison the spectra normalized at 1 should be used. Data from these sub-entries should be divided at k = 1.56 (ratio of nu-prompt values for ^{252}Cf(sf) and ^{235}U(n_{th},f)). This was done for data from Sub-entry 40871011. For data from sub-entries 40871012 and 40872007 were divided at 1.64 and 1.66 respectively, to exclude ratio normalization problems and treat all ratios measured by Starostov *et al.* as shape-type data. The ratio of ^{252}Cf(sf) standard evaluation to ^{235}U(n_{th},f) reference spectra is shown by the thick solid red line.

It is interesting for validation of these ratios to introduce into these figures calculated and evaluated (experimental) results presented by Mannhart for ratio of cross sections averaged on these spectra in dependence from mean neutron energy of their response. The evaluated (experimental) averaged cross sections ratios are shown on these figures by black squares, and calculated averaged cross sections ratios by black dashed line.

The following conclusions can be drawn from these comparisons:

1. The calculated average cross-section ratios in dependence from mean neutron energy of the response are smooth and not sensitive to the particular shape of the reaction cross section.
2. Difference in the ratio of the spectra (thick red line) and calculated averaged cross-section ratios is in the limit of 2 - 3%.
3. Starostov shape of ratios is consistent with standard and reference spectra evaluation with the exclusion of the energy range below 500 keV, where they have different energy dependence.
4. Above 10 MeV the evaluated (experimental) averaged data show that either ^{252}Cf(sf) spectrum is too hard, or ^{235}U(n_{th},f) is too soft, or both trends are present, or evaluated (experimental) ratios on some reasons are too low.
5. Starostov data on shape of ratios of two spectra can be included in the combined fit of ^{252}Cf(sf) and ^{235}U(n_{th},f) prompt fission neutron spectra.

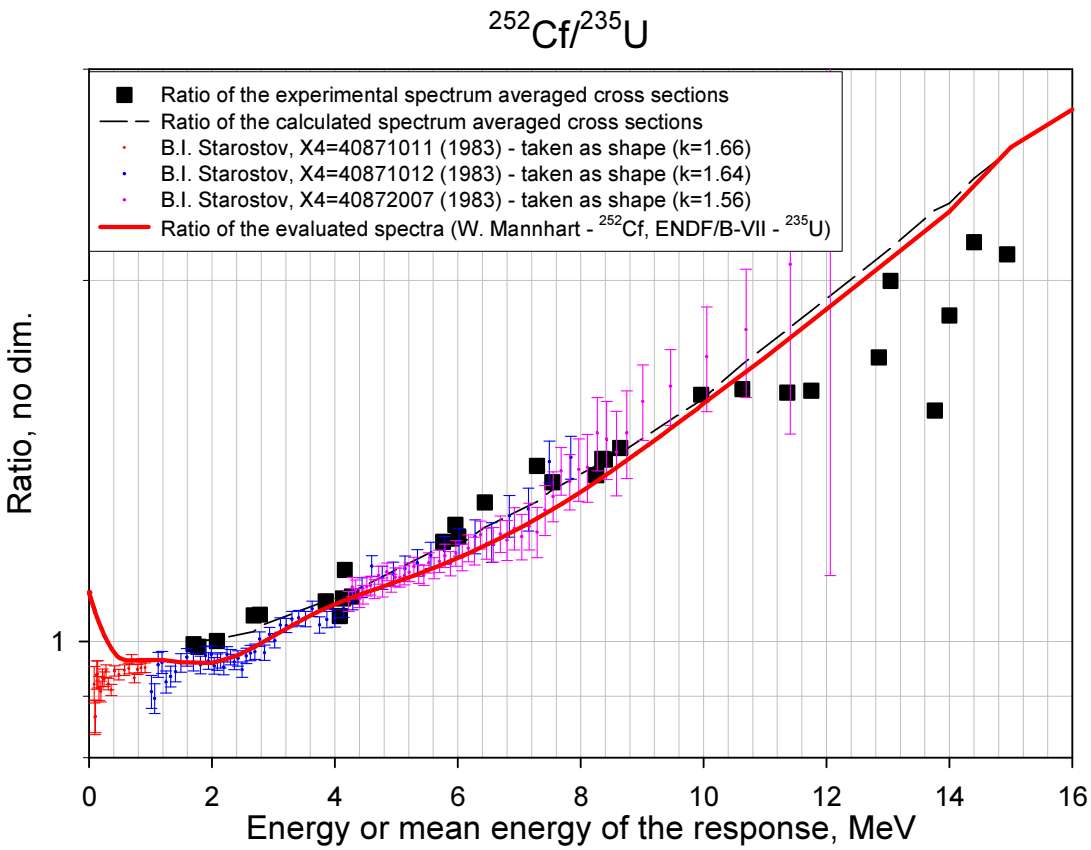

Fig.1. Lin-log presentation (see explanations in the text).

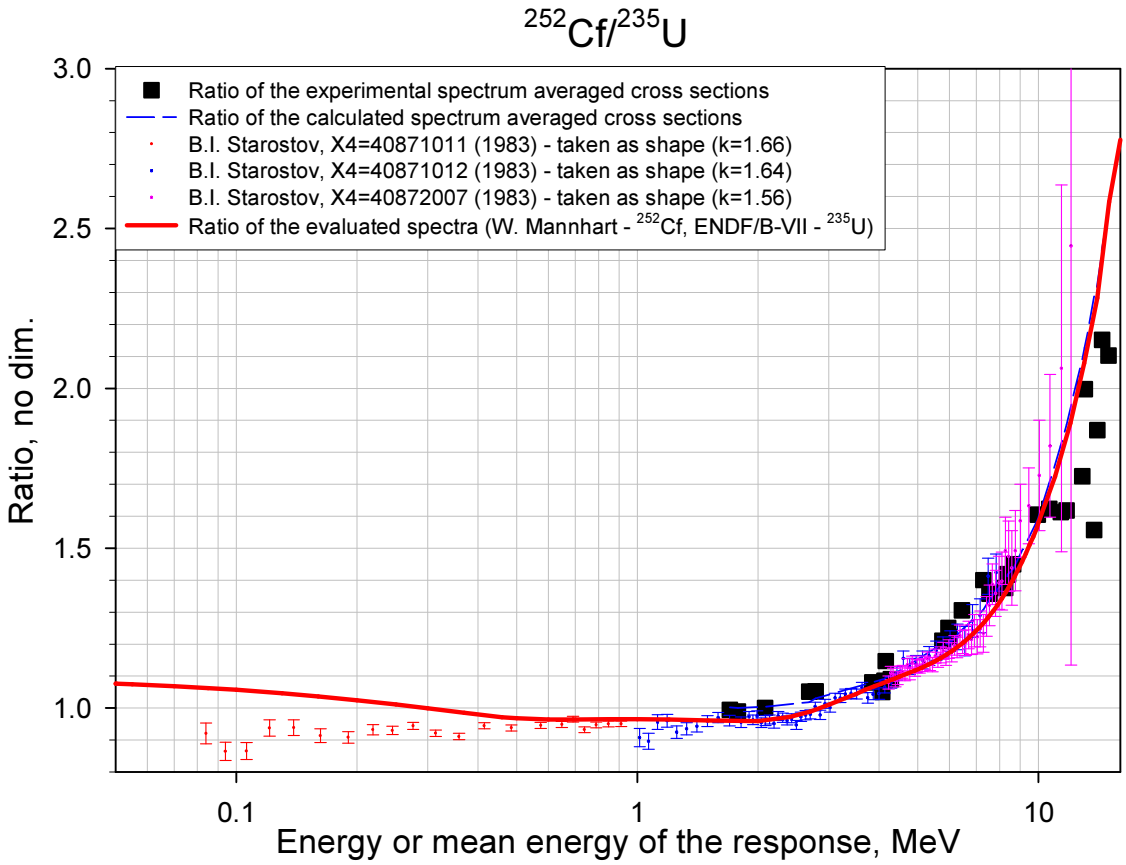

Fig. 2. Log-lin presentation (see explanation in the text).

Recent measurements of the prompt neutron emission spectrum from neutron-induced fission of ^{235}U

Kornilov, N.V., Hambsch, F.-J., Fabry, I., Oberstedt, S.
European Commission JRC-IRMM, B-2440 Geel, Belgium
Simakov, S.P.
Forschungszentrum Karlsruhe, Institute for Reactor Safety, D-76021 Karlsruhe Germany

Following a recommendation of the NEA Working Party on Evaluation cooperation (WPEC) [1] the prompt fission neutron spectrum (PFNS) was measured during three measurement campaigns at an incident neutron energy E_n = 0.5 MeV

1. Experimental procedure and results

During the last years three measurement campaigns took place at the 7 MV Van de Graaff accelerator of the IRMM in Geel, Belgium, to measure accurately the prompt fission neutron emission spectrum at neutron energy $E_n \approx 0.5$ MeV using the fast neutron time-of-flight technique. A pulsed proton beam of about 1.0 - 1.5 ns FWHM at 1.25 - 2.5 MHz repetition rate and 0.2 - 0.8 μA average current was used. Mono-energetic neutrons of 0.52 MeV average energy were produced using the ^{7}Li(p, n) reaction. A metallic ^{235}U sample (93.15 % enrichment, 161.28 g) and a similar sized lead sample were applied for foreground and background measurements, respectively.

In a first run (Jul06) different emission spectra were measured for different emission angles relative to the neutron beam. The neutron yield was ~ 10% and the average secondary neutron energy ~ 80 keV higher at 120^{o} compared to 90^{o}. The result was discussed at the Nice ND2007 conference [2]. This unusual finding stimulated new investigations to verify and to estimate the nature of this effect. In a second experiment (Apr07) we used three identical neutron detectors at a flight path of 2.24 ± 0.01 m placed at 90^{o}, 150^{o} and 120^{o}. The distance from the neutron production target to the sample was ~ 8 cm.

In a third experiment (Jan08) the same detectors were applied. Two of them were placed at 90^{o} to the left (L90) and right side (R90) relative to the proton/neutron beam direction. The third detector was at 150^{o} at the right side. Flight paths were of 2.25 ± 0.01 m. The sample was placed at 8.5 ± 0.2 cm from the neutron target (0^{o} position) and was moved also along the axis between detectors R90 and L90 at ± 3 cm and ± 7 cm. The plus sign means that the sample was moved towards the R90 detector and the minus sign in opposite direction towards the 90L detector. The third detector can see the sample only in the 0^{o}-position. Results for the sample in the 0^{o}-position only are discussed in this report. In every experiment the neutron detectors were shielded against direct and room-scattered neutrons.

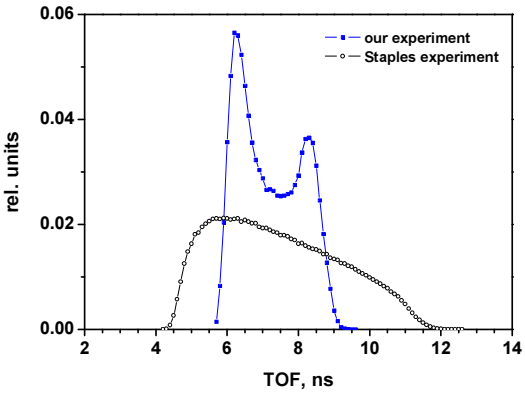

Fig. 1. Comparison between the TOF distribution of the input neutrons inside the sample for the present experiment (full symbols) and the one of Ref. [6] (open symbols). The data are from a Monte Carlo simulation.

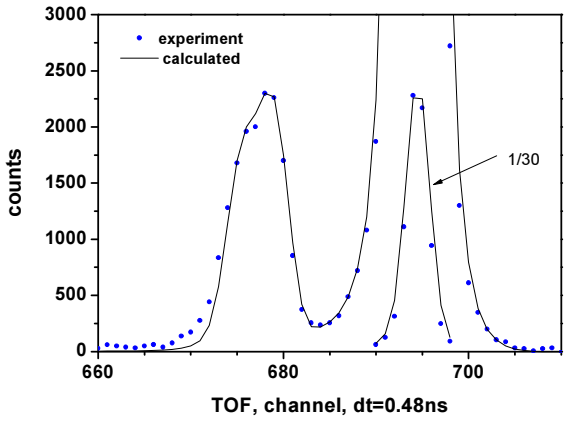

Fig.2 Prompt-gamma ray peaks measured by detector R90 (Jan08 run). The threshold is 1.2 MeVee. The channel width is 0.47 ns. The convoluted result is also given. The target gamma-rays (right) peak gives the detector resolution and proton pulse width. The prompt fission gamma-rays give the total time resolution including neutron spread inside the sample (Fig. 1).

Table 1. Average energies of the PFNS for all angles and runs. The letters shows left-L and right-R sides of the detector relative to the proton/neutron beam, ΔE = 0.010 MeV.

Angle, degree	<E>, MeV Jul06	<E>, MeV Apr07	<E>, MeV Jan08
R90	2.004	2.002	2.021
L90			2.007
L120	2.076	2.050	
R150		2.026	1.975

The traditional pulse-shape analysis was applied to reduce the gamma-ray background. A small Pilot-U scintillation detector was used as proton pulse-shape monitor. The data were collected in list mode for offline analysis. The detector efficiencies were measured relative to the ^{252}Cf standard spectrum. A specially designed low mass, fast ionization chamber [3] was put at the place of the U-sample keeping the same geometry as during the experiments. The energy spectra were corrected for detector efficiency, for neutron multiple scattering in the sample, and for time resolution. A detailed description of the experimental procedure will be published elsewhere [4].

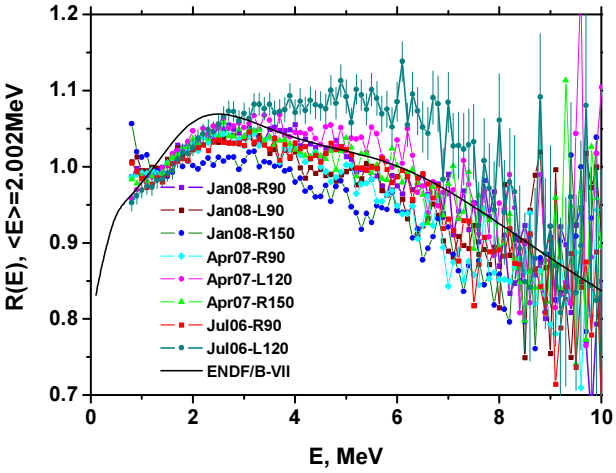

Fig. 3. Comparison between all of our results (full symbols).
The ENDF/B-VII spectrum is given as a full line.

The pulse mode operation of the VdG was not the same during these experiments. The FWHM was ~ 1 - 1.5 ns in all experiment. However, some tailing did exit which could not be removed completely. The worst tailing was observed during the Jul06 experiment. The best beam quality was realized during the third experiment, with a FWHM ~ 1 ns and a FW(1/1000)M < 10 ns. We recalculated the time resolution correction for the measured spectra from Jul06 published before [2, 5].

Additional energy dependence in the neutron detector efficiency at E > 4 MeV has been taken into account, too. This factor slightly reduced the PFNS in the energy range 5 - 8 MeV and the average secondary neutron energy by up to ~ 15 keV for the first run.

The time resolution of the TOF spectrometer consists of the following components: detector resolution, pulse shape of the accelerator and neutron distribution inside the sample. The last factor is very important. Fig. 1 shows the TOF intensity distribution of the incident neutrons inside the sample for our experiment compared to the one in Ref. [6]. Clearly the double peaked intensity structure of our ring shaped sample is visible in contrast to the very broad distribution of the very large sample (7.7 cm diameter) of Ref. [6]. This factor together with a shorter flight path (1.63 m) in spite of a very short proton burst of 0.6 ns in Ref. [6] is very important for data comparison. Therefore, the experimental data of Ref. [6] were corrected for this time resolution assuming the same contribution of the detector resolution as in our experiment. The present experimental time resolution together with the calculated dependences including all factors is given in Fig. 2.

The experimental PFNS were normalized to unity and the average secondary neutron energy was calculated. A Maxwellian spectrum was fitted in the energy range of 0.7 - 1.5 MeV and 9 - 11 MeV to the measured spectrum and an extrapolation to zero and to 20 MeV was done. Based on our detailed analysis of all incorporated corrections and possible uncertainties, we conclude that the average energy is estimated with an accuracy of ± 0.010 MeV. The average energies measured in all experiments are given in Table 1.

The PFNS at all investigated angles and for all runs are shown in Fig. 3 as a ratio to a Maxwellian distribution with the average energy <E> = 2.002 MeV. The following peculiarities may be highlighted:

1. The data demonstrate the variety of the spectrum shape. A difference exists not only for various detector angles but for detectors at 90 degree placed at left and right sides (see Jan08 90R, 90L in Fig 2 and Tables 1, 2);

Table 2. Average spectral ratios <R> = N(E, 90R)/N(E, 90L) and corresponding uncertainties for different energy intervals.

E_1-E_2, MeV	<R> ± δR	E_1 -E_2, MeV	<R> ± δR
0.8 - 2	0.999 ± 0.003	5 – 6	1.009 ± 0.005
2 - 3	1.010 ± 0.002	6 – 8	1.051 ± 0.006
3 - 4	1.020 ± 0.005	8 – 10	0.970 ± 0.032
4 - 5	1.034 ± 0.004		

2. The normalized spectra are fixed at low and high energies (see Fig. 3). The integrals between 1.3 - 2.3 MeV and 8 – 10 MeV are constant. The standard deviations of 8 spectra are 0.2 % and 3 %, respectively;

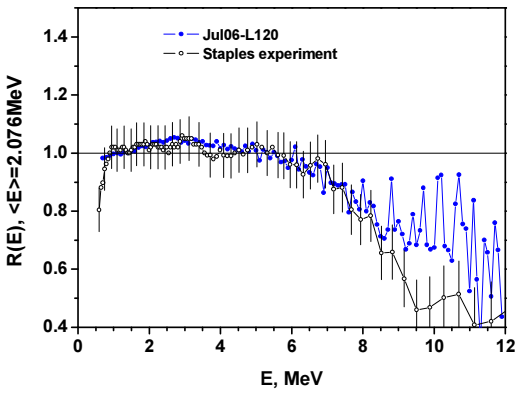

Fig. 4. Comparison between our result (Jul06 L120 detector) and data from Ref. [6].

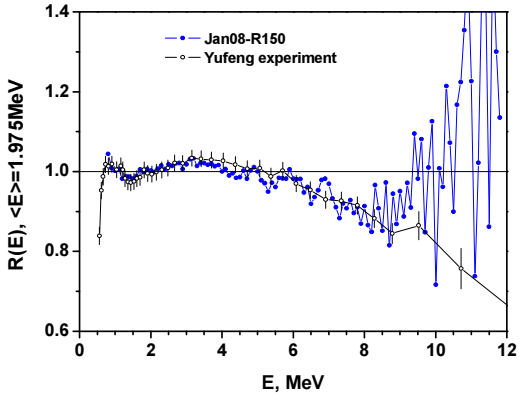

Fig.5. Comparison between our result (Jan08, R150 detector) and data from Ref. [7].

3. Among the data one may find a result which agrees perfectly with an old experiment or evaluation.

A comparison between the different experiments and literature values are given in Figs. 4-8. The spectra measured at thermal energy were normalized to a Maxwellian with reduced average secondary energy - $\langle E_{th} \rangle = \langle E_{0.5} \rangle * 0.995$.

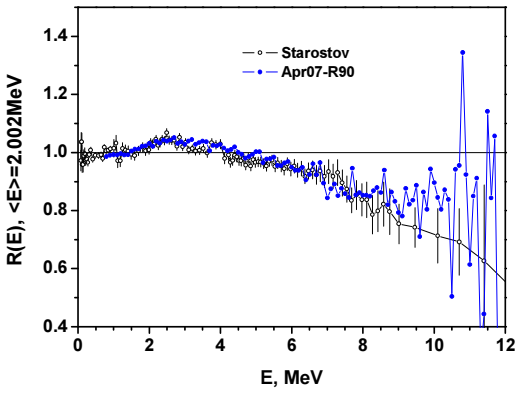

Fig. 6. Comparison between our result (Jul06, R90 detector) and data from Ref. [8].

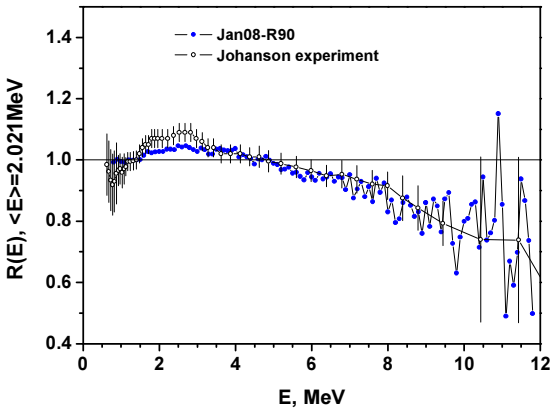

Fig. 7. Comparison between our result (Jan08, R90 detector) and data from Ref. [9] corrected with multiple scattering and angular distribution from the T(p, n) reaction taken from Drosg's evaluation [10].

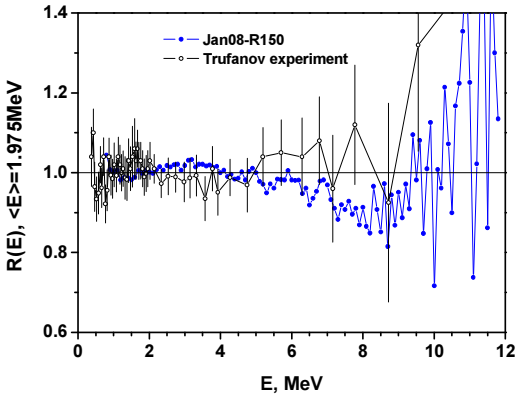

Fig. 8. Comparison between our result (Jan08, R150 detector) and data from Ref. [11].

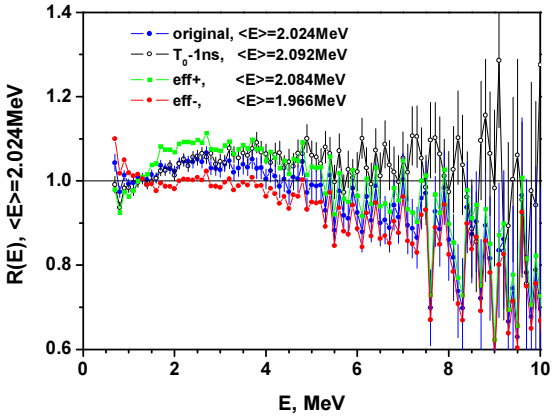

Fig. 9. The original spectrum and the ones estimated using different perturbation factors as given in the legend.

Before starting any scientific discussion about the nature of this strange behavior of the PFNS one should answer the main question: is this a real effect or an experimental artifact?

2. Possible experimental problems

The experiments were carried out relative to the standard ^{252}Cf spectrum measured in the same experimental conditions. Therefore a lot of systematic uncertainties such as: flight path, uncertainties in the time channel width, a possible time reference shift (T_0 value) connected with the detector operation, a distortion of the spectrum due to scattering in the collimator are drastically reduced or even canceled.

The shift of T_0 versus pulse height was investigated. After an additional correction as a function of pulse height, the shift was < 0.1 ns (ADC channel width was 0.117 ns).

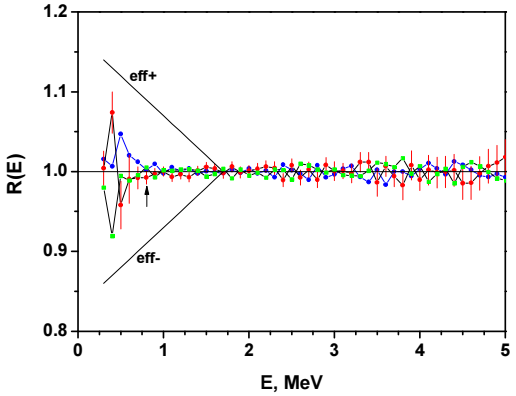

Fig. 10. The ratio of the detector efficiencies to the average value measured during the Jan08 experiment at the beginning, in the middle and at the end of the experiment. The distortion factors are shown by the full line. An arrow shows the cut-off energy in the data analysis.

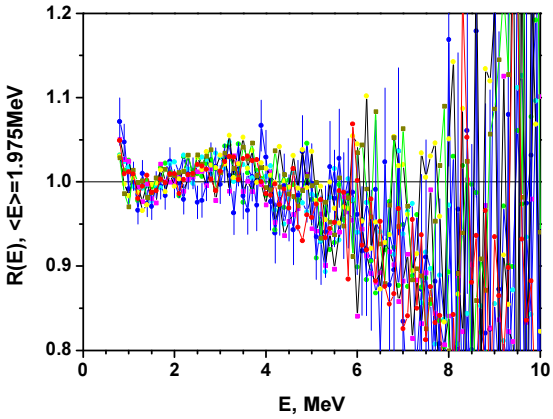

Fig.11. The spectra measured by the R150 degree detector during the Jan08 run.

We investigated a possible change of the ^{252}Cf spectrum due to different emission angles of the neutrons relative to the electrode plates in the ionization chamber. The ionization chamber was rotated relative to its vertical axis and the neutron spectra were measured by two detectors at 90°, and 120° [4]. No influence was found.

The spectrum shape may be distorted due to the proton pulse shape (VdG pulse mode operation) and a possible mistake in the time resolution correction. In this case the high energetic part of the spectrum (most sensitive to the time resolution) should be distorted. Since we observe the same integrals for the energy interval 8 - 10 MeV this argument is not valid. In addition, this factor is common to all detectors and cannot explain the observed difference between them.

So the most sensitive factor is the stability of the detectors and the correct estimation of the T_0 value. The detector efficiency might be arbitrary changed in between the Cf and U measurements. As one can see in Fig. 2 the prompt fission peak (the zero time (T_0) is determined relative to the prompt peak position) is very well separated from the main component due to prompt gamma rays from the target and T_0 can be deduced with an accuracy of ~ 0.1 ns. In addition to provide a measureable difference between the spectra we should shift T_0 in the opposite direction relative to the neutron detector.

We simulated the influence of both factors. The results are given in Fig. 9. We calculated the spectrum with the nominal parameters, with a shifted T_0 by 1 ns and with a distorted detector efficiency by the function $1 \pm 0.1 * (1.7 - E)$, $E < 1.7$ MeV. The influence of these factors may provide an effect comparable with the data spread shown in Fig. 3, the average secondary energy varied by ± 70 keV. However, a shift of T_0 by 1 ns changed the integral in the energy range 8 – 10 MeV by 28 % which is ~ 10 times higher than the real data spread visible in Fig. 3. Therefore, we may also exclude this.

Another possibility would be that the distortion factor is connected with instabilities of the threshold and neutron-gamma discrimination parameters. The detector efficiencies were measured before, in the middle, and after the U run in each experiment. The U-spectra shown in Fig. 3 are sums of several (5-7) runs measured during 10 - 20 hours, so the direct comparison of the separate spectra may answer this question about the detector stability. According to the results given in Figs. 10 and 11 there is no evidence for any notable detector instability, which might have resulted in the observed variation. In addition, the detector efficiencies were in very good agreement with calculated results using the NEFF7 code [12], see Fig. 12.

These arguments are valid for each of the experiments, and the present conclusion is that we measured a real effect with respect to all possible, i.e. known, systematic error sources inherent in the present experimental approach!

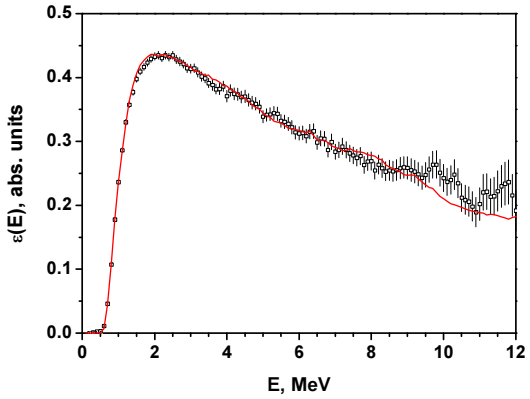

Fig. 12. The efficiency of one detector (Jan08, R150 detector) measured relative to ^{252}Cf and calculated with the NEFF7 code (full line).

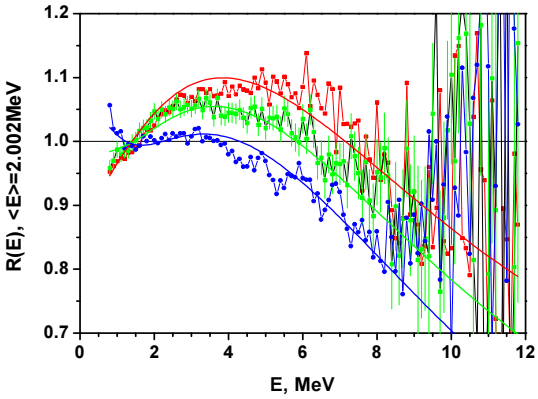

Fig.13. Some experimental data and their description with a "3 source model". Blue line - $\zeta = 0.6$, green – $\zeta = 0.4$, red – $\zeta = 0.2$ (for details see text).

3. What does this experimental fact mean?

On the basis of the above discussion one may conclude that a factor exists which has a rather strong influence on the PFNS shape and asymmetry effects but was not fixed in our investigations and in all available experiments performed during the long history of fission investigations. One may assume for example, that this factor is connected to the neutron source, pointing to an angular anisotropy caused by neutron polarization. In the preparation stage of any PFNS experiment it was assumed that this factor is not important or, by definition, should be equal to zero. If this explanation is true, the transmission mechanism of the information from the incident neutron to the secondary fission neutron should be found. The only possibility might be (pre-) scission neutron emission, a fast process without formation of the compound nucleus. This may provide the link between the incident neutron and the secondary fission neutron. We should have in mind that three particles (two fission fragments and a scission neutron) are emitted at the same time which complicates the problem a lot.

The information about scission neutron emission is very poor. It was estimated in Ref. [13] that the probability of fission with scission neutron emission is ~ 40 % (which corresponds to

a total of 15 % in total multiplicity), that the spectrum of scission neutrons consists of a low (~ 0.8 MeV) and a high (~ 2.5 MeV) energy component. In Ref. [14] evidence was given that scission neutrons are emitted by fission fragments with high total kinetic energy (TKE) (compact system). From the results of this paper we may estimate a high energy limit in the spectrum for scission neutron emission of ~ 8.5 MeV. The questions is now, which parameters should be changed to provide the variety of results given in Fig. 3.

In case of scission neutron (SCN) emission, fission neutrons should be emitted from three sources:

1. Neutrons from fragments after fission of the compound nucleus $A+1$

$$N_{A+1}(E) = (1-\alpha)\cdot W_{A+1}(E)\,, \qquad (1)$$

where α is the share of scission neutron emission and W_{A+1} is the spectrum which describes the neutron emission from accelerated fragments;

2. Neutrons from accelerated fragments after fission of the nucleus A, which is formed after the emission of one SCN:

$$N_{A}(E) = \alpha\cdot(\nu-1)\cdot W_{A}(E)/\nu\,. \qquad (2)$$

3. Scission neutrons itself:

$$N_{scn}(E) = \frac{\alpha}{\nu}\cdot E\cdot\left(\frac{\varsigma}{T_1^2}\exp\left(-\frac{E}{T_1}\right)+\frac{1-\varsigma}{T_2^2}\exp\left(-\frac{E}{T_2}\right)\right), \qquad (3)$$

where ζ is the share of the low energy component and ν is the neutron multiplicity.

The spectra W_A, W_{A+1} were calculated with a Watt distribution for light and heavy fragments with masses $A_h = 140$ and $A_l = A\text{-}140$. The ratio of the neutron multiplicity for light and heavy fragments was $\nu_l/\nu = \nu_h/\nu = 0.5$. Temperature parameters were found based on the Fermi-gas relation and the thermal-equilibrium assumption with an additional correction of cor = 0.9 for the excitation of the heavy fragment $U_h = U_{0h} \cdot$ cor [13]. The level density parameter was calculated as $a = A/c$, c = 8.4, TKE = 170.5 MeV, ν = 2.45.

The equation for $N_{scn}(E)$, and the corresponding parameters T_1, T_2 were taken from Ref. [13] introducing minor corrections: $T_1 = 0.4$ MeV, $T_2 = 1.35$ MeV. Changing only ζ from ζ = 0.2 to ζ = 0.6 allowed us to describe the spectrum shape with reasonable accuracy from the highest average secondary neutron energy $\langle E\rangle$ = 2.070 MeV to the lowest $\langle E\rangle$ = 1.967 MeV (Fig.13). The spectrum with ζ = 0.31 extrapolated to thermal energy describes the integral experiments. The average ratio of the calculated cross sections to the experimental ones (Ref. [15], IRDF-2002) is $\langle R\rangle$ = C/E = 0.997 ± 0.008. The average energy of the PFNS at thermal energy is $\langle E\rangle$ = 2.038 MeV.

4. Conclusion

In conclusion, a very unusual result, not observed before was found in the present investigation. The variation of the experimental prompt neutron spectra with emission angle relative to the proton/neutron beam cannot be explained with any model. Therefore, it is suggested to assume that a different mechanism of the fission process and of neutron emission should be incorporated.

For the moment we may only conclude, that the measured effect is not an experimental

artefact. We should assume the existence of an additional factor (parameter), for example the neutron polarisation, which might be responsible for the measured peculiarities. Therefore, new experimental efforts are urgently needed. It seems experiments with polarised thermal neutrons would be very interesting.

References

1. Madland D.G., ISBN-92-64-02134-5, NEA/WPEC-9, 2003.
2. N.V. Kornilov, F.-J. Hambsch, I. Fabry, et al., *Proc. of the Int. Conf for Nucl. Data for Sci. and Tech., ND2007,* Nice, France, Apr 2007, 387, DOI: 10.1051/ndata:07735.
3. N.V.Kornilov, F.-J. Hambsch, S. Oberstedt et al., JRC-IRMM, Neutron Physics Unit, Scientific report 2005, p. 67.
4. N.V. Kornilov, F.-J. Hambsch et al., Internal report GE/NP/01/2007/02/14.
5. N.V.Kornilov, F.-J. Hambsch, S. Oberstedt et al., JRC-IRMM, Neutron Physics Unit, Scientific report 2006, p. 37.
6. P. Staples, J.J. Egan, G.H. R. Kegel, A. Mittler and M.L. Woodring**,** Nuclear Physics **A591** (1995) 41.
7. W. Yufeng et al., Chin. J. Nucl. Phys. **11** (1989) 47. EXFOR32587.
8. B.I. Starostov et al., Nejtronnaja Fizika (6-th Conf. for Neutron Phys., Kiev. 1983), 1984. T.2. C.285,290, 294, EXFOR 40871, 40872, 40873.
9. P.I. Johansson, B. Holmqvist, Nucl. Sci. Eng. **62** (1977) 695.
10. M.Drosg, http://www-nds,org/drosg2000.html.
11. A.M. Trufanov et al., J. Nucl. Phys. **57** (1994) 606.
12. G. Dietze, H. Klein, PTB-ND-22 Report (1982).
13. N.V. Kornilov et al., Phys. of At. Nucl. **62** (1999) 209 and Nucl. Phys. **A686** (2001) 187.
14. N.V.Kornilov, F.-J. Hambsch, A.S. Vorobyev, Nucl. Phys. **A789** (2007) 55.
15. K.I. Zolotarev, INDC(NDC)-448, 2003, 25.

Measurements of Angular and Energy Distributions of Prompt Neutrons from Thermal Neutron-induced Fission of $^{235}U(n_{th}, f)$

A.S. Vorobyev, O.A. Shcherbakov, Yu.S. Pleva, A.M. Gagarski, G.V. Val'ski, G.A. Petrov, V.I. Petrova, T.A Zavarukhina
Petersburg Nuclear Physics Institute, 188350, Gatchina, Leningrad district, Russia

Introduction

By now, a large number of theoretical and experimental works have been performed to study the prompt neutrons emission mechanism in fission. In spite of a significant advance in the understanding of this process a long standing question remains without answer: there are or not the neutrons in low energy fission which are emitted from not fully accelerated fragments [1]? Up to now the prompt fission neutron spectra are evaluated on the base of semi-empirical systematic where a deficiency of knowledge about neutron emission mechanism is compensated by adjustment of model parameters. Therefore the predictive power of this model is very limited and constrained for nuclides and energy region for which no data exist.

From the experiments performed earlier for ^{235}U it should be expected to obtain the highest relative yield of neutrons emitted not from fully accelerated fragments. Due to the fact that it was suggested to use ^{235}U as a neutron standard, the clarification of neutron emission mechanism becomes a very important problem.

Only the investigations of the fission neutron angular and energy distribution relative to the fragment direction depending on mass split and fragment kinetic energy gives possibility to estimate the yield of neutrons with the formation nature other than evaporation from fully accelerated fragments. The measurements at 11 fixed angles between the neutron and light fragment directions in the range from 0^0 to 180^0 in 18^0 intervals were performed recently at the PNPI RAS. In the present paper we present first results.

1. Experiment overview

The measurements were carried out at the radial neutron beam N7 of the research reactor WWR-M of the PNPI RAS in Gatchina equipped with a neutron guide 3 m in length. The flux density of neutrons of wavelength $\lambda \sim 1.5$ Å from the neutron guide outlet slit (3 x 40 mm^2 in cross-section) was $\sim 2 \cdot 10^7$ $cm^{-2} \cdot sec^{-1}$. The measurements were carried out in weekly cycles. The data accumulated over each cycle were processed separately.

The fission fragments and prompt neutrons time-of-flights were measured simultaneously for 11 fixed angles between the neutron and light fragment directions in the range from 0^0 to 180^0 in 18^0 intervals. The schematic view of the experimental set-up is shown in Fig. 1. The neutron beam was coming along the chamber axis normally to the picture plane. It should be noted that realized scheme of experimental set-up guarantees identity of conditions of the neutron spectra measurements at various angles relative to the fission axis, namely: the magnitude and composition of the background, the efficiency of the neutron detectors, and neutron re-scattering by the parts of experimental set-up. Also, using two neutron detectors with slightly different characteristics allows estimate probable systematic errors of the data obtained.

The prompt neutrons were detected using two stilbene crystal detectors (Ø 50 mm x h 50 mm and Ø 40 mm x h 60 mm) positioned with a 90^0 angle between their respective axes at a distance of 47.2±0.2 cm and 49.2±0.2 cm, respectively, from the fissile target. The neutron registration threshold was 150 – 200 keV. To separate events corresponding to neutrons and γ-quanta, a double discrimination by the pulse shape and the time-of-flight was applied. The full time uncertainties were defined from FWHM of the "fragment - γ-quantum" coincidence curve which was equal to 1.2 ns.

Fig. 1. Schematic view of the experimental setup (no scale).

The fission fragments were detected by multi-wire proportional detectors (MWPDs) in conjunction with the TOF technique. The 16 rectangular fragment detectors were located in the form of 2 arcs (8 detectors in every one) diametrically opposite each other in the reaction chamber at the operating gas (isobutane) pressure of 4 ÷ 6 Torr. A detail description of the experimental set-up can be found in Ref. [2].

As a result, the energy distributions of prompt neutrons emitted from fixed pair of fission fragments were obtained. During data processing, the following corrections were taken into account: for detector efficiency, for neutron detector background, for angular and energy resolution, for the fragment detector efficiency and for complementary fragment contribution. The detector efficiency was determined by comparing the total (in present experimental set-up it corresponds to the neutron yield integrated over all angles) neutron energy spectrum in laboratory system with the evaluated total neutron spectrum ^{235}U from Ref. [3].

2. Simple evaporation model

It is well established that the prompt neutrons in low energy fissions are emitted mainly from fully accelerated fragments and the yield of neutrons with other emission mechanism may range from 1% to 20% of the total prompt neutron yield. The wide scatter of the published data on such neutron yield is caused probably by the different shape of the neutron spectrum in the center-of-mass system used in analysis. This follows as the yield of these neutrons is usually determined by comparing experimentally observable variables in the laboratory system with those calculated using known center-of-mass spectra on the basis of the assumption that neutrons are emitted only from fully accelerated fragments. We used a more constitutive approach which consists in obtaining the neutron spectrum in the center-of-mass system without resort to any model representation, using only experimental data for small angles relative to the fission direction.

A circumstance of considerable importance is the fact that in these cases it is possible to obtain a neutron spectrum in the center-of-mass system, which is practically unrestricted in the low energy range. Admittedly, in this case not only the response function is produced but also the neutron yield in absolute units.

In the first step of calculations, it was assumed that neutrons registered at 0^0 and 180^0 angles were emitted solely by the light and heavy fragments, respectively. In the second step, the neutron contribution to the complementary fragment was subtracted (Fig. 2).

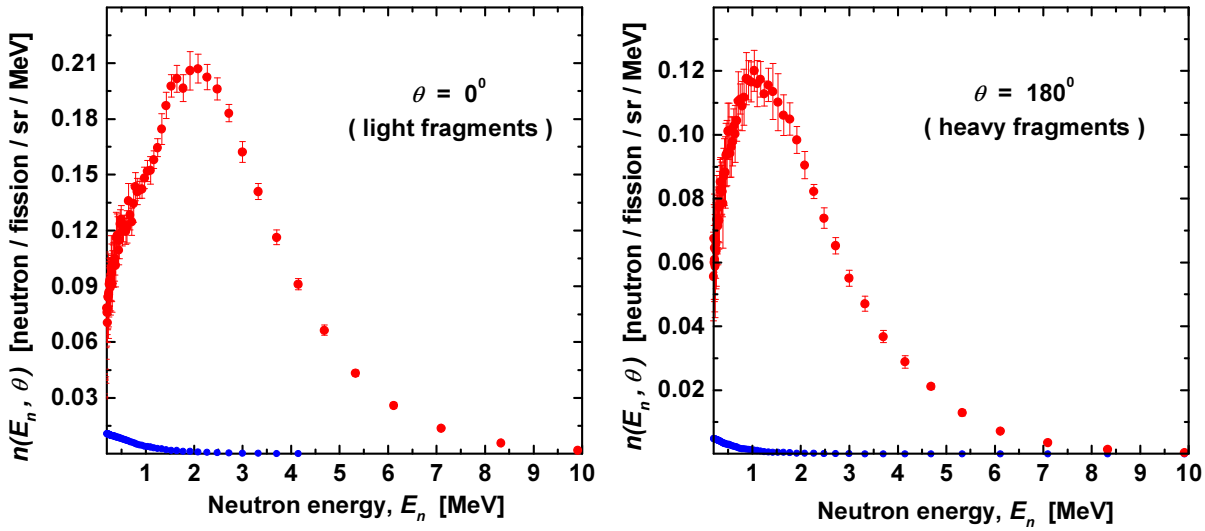

Fig. 2. Spectrum of fission neutrons in laboratory system: experiment –circles with error bars; model calculation (contribution of fission neutrons from complementary fragment) –circles without error bars.

Then, using the energy spectra for 0^0 and 180^0 angles obtained in this way in the laboratory system, the neutron energy spectra for light and heavy fragments were obtained in the center-of-mass system. While doing so, it was assumed that the specific energy per nucleon for light and heavy fragments, respectively, was $E_L = 1.025$ MeV and $E_H = 0.476$ MeV. The reference spectra obtained in the center-of-mass system (Fig. 3) were used for calculation of neutron energy and angular distributions in the laboratory system:

$$n_{lab}(E_n, \Omega) = (E_n / E_{c.m.})^{1/2} \cdot \varphi(E_{c.m.}, \Omega_{c.m.}) \cdot n_{c.m.}(E_{c.m.}, \Omega_{c.m.}), \quad (1)$$

$$\varphi(E_{c.m.}, \Omega_{c.m.}) = 1 + A_2 \cdot E_{c.m.} \cdot (3 \cdot \cos^2(\Omega_{c.m.}) - 1) / 2, \quad (2)$$

where the function $\varphi(E_{c.m.}, \Omega_{c.m.})$ is the angular distribution of neutrons in the center-of-mass system and the parameter A_2 defines the value of the angular anisotropy; $n_{lab}(E_n, \Omega)$ and $n_{c.m.}(E_{c.m.}, \Omega_{c.m.})$ are the corresponding neutron yields in laboratory and center-of-mass system, per unit energy range and solid angle; E_n, Ω and $E_{c.m.}$, $\Omega_{c.m.}$ are the energy and angle in the laboratory system and center-of-mass system.

Due to the fact that fission fragments possess an angular momentum leading to neutron emission anisotropy in the center-of-mass system, the equations (2) describing the neutron emission by fission fragments formally enclose a possibility of anisotropy characterized by the anisotropy coefficient A_2. As a first approximation, a model of isotropic neutron emission was used, that is $A_2 = 0$.

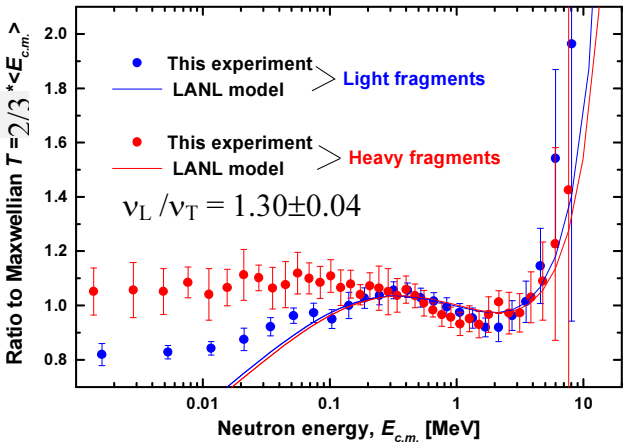

Fig. 3. Ratio of the prompt fission neutron spectrum from light and heavy fragments in the center-of-mass system to the Maxwellian spectrum with adjusted parameters ($<E^{L}_{c.m.}>$ =1.17±0.3 MeV, $<E^{H}_{c.m.}>$=1.26±0.2 MeV).

LANL model [4]:

neutrons are evaporated by fully accelerated fragments;

average velocities and masses of light and heavy fragments are used in calculation;

the cross section for the inverse process of compound-nucleus formation is constant.

3. Results and discussion

The number of fission neutrons and their average energy for fixed angles in the laboratory system (obtained experimentally and calculated using an assumption about isotropic emission from fully accelerated fragments) are shown in Figs. 4, 5. Both experimental and model neutron spectra have been compared in 0.2–10 MeV energy range. The errors of the obtained experimental data are comparable with the point's size. In these figures, the experimental results of K. Skarsvag and K. Bergheim [5] are also shown. These authors came to a conclusion that about 15% of neutrons are emitted during the fission process itself. In our case, on the whole, the calculated model energy and angular distributions agree rather well with the experimentally obtained distributions.

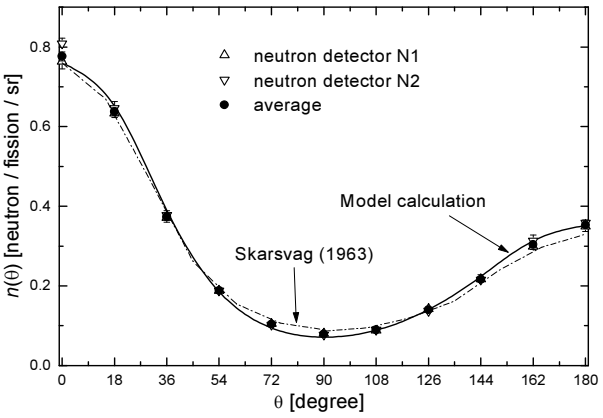

Fig. 4. Fission neutron yield as a function of the angle between neutron exit direction and the direction of motion of the light fragments.

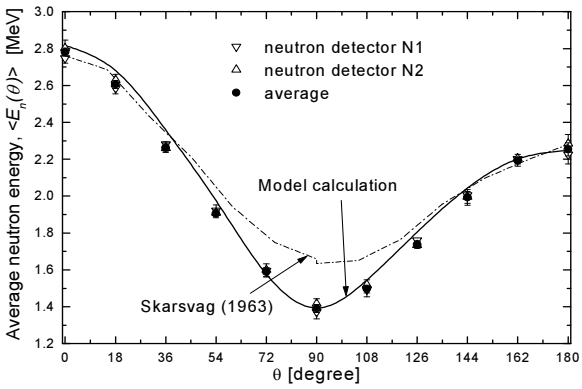

Fig. 5. Angular dependence of the average neutron emission energy in the laboratory system.

However, there is a minor distinction which is most clearly demonstrated in Fig. 6, where it is shown the angular dependence of the ratio of experimentally obtained neutron yield to calculated one. A maximal difference between the model calculation and the experiment is ~ 10% for the angles near 90^0. For the total spectra (integrated over all angles) this difference does not exceed 5% therewith. The sensitivity of model was evaluated by using different value of energies per nucleon for the heavy (0.47-0.49 MeV) and light (1.01-1.04 MeV)

fragments. It was found that the ratio value (Fig. 6) at 90-deegre changes in the interval 1.09-1.12, that is within the experimental uncertainties. Obviously, the ratio of the spectra in polar and equatorial direction is a very sensitive to some variation of an emission mechanism. The energy dependence of the ratio of neutron yields measured at 0^0 and 90^0, as well as that at 180^0 and 90^0, is shown in Fig. 7. The measured ratio is in a good agreement with rough evaporation calculation at high energy region and we conclude that there is not any unambiguous argument of the existence of other mechanism of neutron emission.

Special attention must be given to the fact that for angles $\sim 30^0$ and $\sim 150^0$ the model calculation gives overestimated values of fission neutron yield as compared with the experiment. Such a discrepancy, as our model calculation shows, may be related to presence of anisotropy of the fission neutron angular distribution in the center-of-mass system ($A_2 \approx 0.02 \div 0.08$). For example, introduction of anisotropy with $A_2 = 0.04$ into the model calculation leads to an increase in the neutron yield ratio from ~10% to ~15% for angles close to 90^0. At that, the whole integrated spectrum in the energy range above 2 MeV is described with a $\chi 2$ – value close to 1.0 but in the energy range 0.3 – 2 MeV the description is worse.

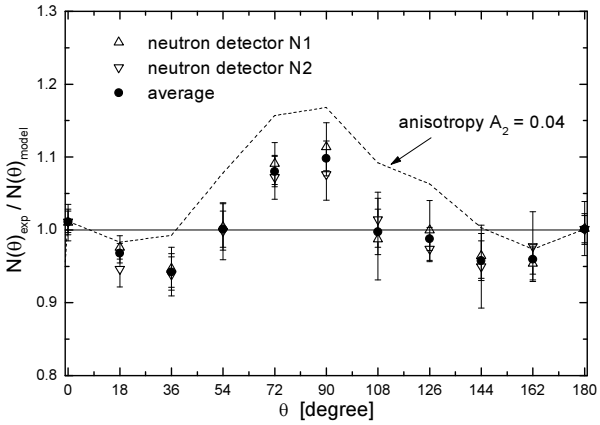

Fig. 6. Angular dependence of experimental and calculated fission neutron yields.

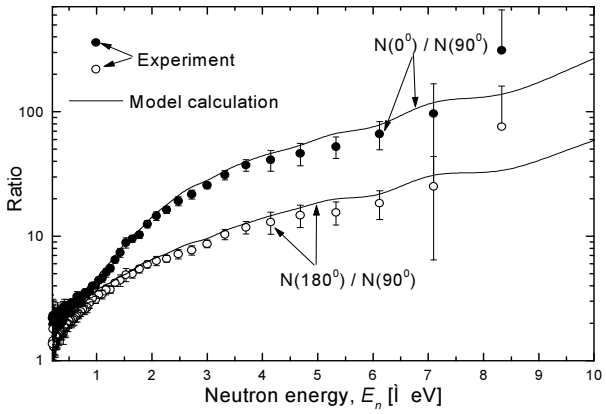

Fig. 7. Ratio of the fission neutron yields as a function of neutron energy for angles 0^0, 180^0 and 90^0 in the laboratory system.

Due to the fact that we are considering the neutron spectrum ratio, our conclusion about the discrepancies between measured and calculated prompt neutron yields, in a systematic sense, is weekly dependent (~3% in equatorial emission) on the choice of the standard neutron spectrum used for calibration of neutron detectors. We obtained this value numerically by using various standard neutron spectrum shapes (Watt distribution, LANL model [4], Kornilov – Ref. [3], Maxwellian). But 3 % is actually a big value, that is why we plan to improve situation by conducting new measurements. When it will be possible to receive a thin ^{252}Cf neutron source, we could repeat calibration of our neutron detectors with this source.

Within the frame work of our hypothesis, the neutron yields have been calculated as a function of the fragments characteristics (Fig. 8, 9). An average number of neutrons obtained for fission event were found to be about 3% lower than a recommended value, that supports a conclusion made above. At that, no difference is observed between the total numbers of neutrons. This fact, probably, is an evidence of absence of any other mechanism besides the evaporation.

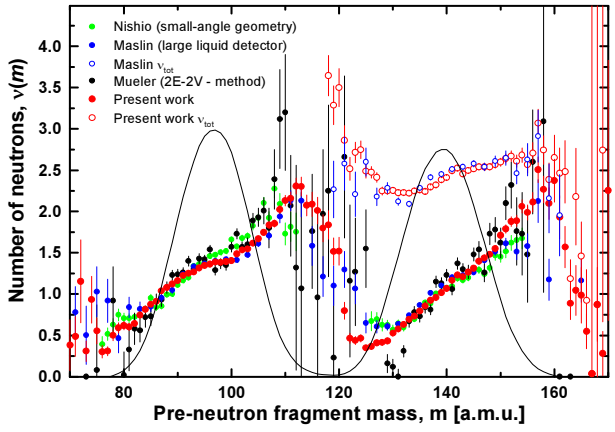

Fig. 8. The neutron yields as function of pre-neutron fragment mass for ^{235}U(n$_{th}$, f) as well as pre-neutron fission fragment mass distribution obtained by these measurements.

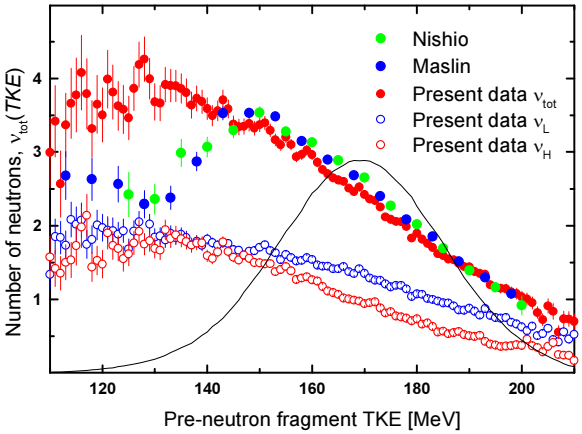

Fig. 9. The neutron yields as function of pre-neutron fragment TKE for ^{235}U(n$_{th}$, f) as well as pre-neutron fission fragment TKE distribution obtained by these measurements.

We observed that for decreasing TKE the neutron yield increases as expected by energy conservation. This is at least true down to energies of 130 MeV. For lower energies our neutron yields are roughly constant. Most probably, the constancy is simply due to the scattered events since at these energies the count rate is extremely low and a few scattered events will have a big influence. This interpretation is underlined by the results of Nishio [6] and Maslin[7]. Their experiments, probably, suffer from some common systematic drawback which caused below about 150 MeV an "anomaly" in conflict with the energy conservation.

4. Conclusion

The energy spectra and angular distributions of fission neutrons have been measured for thermal neutron-induced fission of ^{235}U. A comparison of the measured angular distribution of the ^{235}U(n_{th}, f) fission neutrons with calculation using the model of isotropic emission of neutrons from fully accelerated fragments shows that in the integral spectra a difference in the neutron yield, which could be assigned to a contribution of “scission” neutrons, does not exceed 5%, while a maximum effect is ~10% at the angles near 90^0. Introduction of anisotropy of the fission neutron angular distribution in the center-of-mass system of fission fragments into the model calculation leads to an increase discrepancy with obtained experimental data.

The shape of the neutron spectrum and the number of neutrons obtained in the center-of-mass system both depend on the fragment velocities. As an evaluation, one can use a spectrum written in the center-of-mass system treating the case of two fragments characterized by the average parameters. Taking the example of ^{252}Cf, it was shown by Madland [8] that a transition from the velocity distributions of fragments to the model of two fragments with average parameters has only a minor influence (~ 2%) on the total neutron energy distribution.

It is necessary to perform a complete self-consistent analysis of neutron energy and angular distributions for each fixed pair of fission fragments which should be analogous to that carried out above under approximation of two fragments with average parameters. Only in that case one has a chance to determine for sure a degree of difference between calculated and measured distributions and by this way to clarify a mechanism of neutron emission.

References

[1] G.A Petrov, p.205 in Proc. 3rd Int. Workshop on Nuclear Fission and Fission Product Spectroscopy, 11-14 May 2005, Chateau de Cadarache, Saint Paul lez Durance, France, AIP Conference Proceedings, Vol. 798, 2005, Issue 1,.

[2] A.S. Vorobyev, O.A. Shcherbakov, Yu.S. Pleva, A.M. Gagarski, G.V. Val'ski, G.A. Petrov, V.I. Petrova, T.A. Zavarukhina, Nucl. Instrum. Methods **A598** (2009) 795-801.

[3] N.V. Kornilov, A.B. Kagalenko and K.I. Zolotarev, in: A.M. Sukhovoj (Ed.), VI International Seminar on Interaction of Neutrons with Nuclei "Neutron Spectroscopy, Nuclear Structure, Related Topics", ISINN-6, Dubna, May 13-16 1998, JINR, Dubna, E3-98-202, 1998, p.242.

[4] D. G. Madland and J.R. Nix, Nucl. Sci. Eng. **81** (1982) 213.

[5] K. Skarsvag and K. Bergheim, Nucl. Phys. **45** (1963) 72.

[6] K. Nishio, Y. Nakagome, H. Yamamoto, I. Kimura, Nucl. Phys. **A632** (1998) 540-558.

[7] E. E Maslin, A. L. Rodgers, Phys. Rev. **164** (1967) 1520.

[8] D.G. Madland, IAEA Report INDC(NDS)-251, Vienna, 1991, p.201.

A Note on the Effect of Angular Anisotropy of Neutron Emission in the Fragment Center-of-Mass System

Takaaki Ohsawa
Faculty of Science and Engineering, Kinki University, Higashi-Osaka, Japan

1. Introduction

It is considered from many experimental evidences that fission fragments have high angular momentum of 7 - 8ħ perpendicular to the fission axis due to strong Coulomb torque at the scission point. This leads to anisotropic neutron emission in the fragment center-of-mass (CM) system. Vorobyev suggested in this meeting that this anisotropy may have an effect on the prompt neutron spectrum. A preliminary result of examination of this effect is briefly described here.

2. Equations

The laboratory energy of a neutron E is given by the equation

$$E = E_f + \varepsilon + 2(E_f\varepsilon)^{1/2}\cos\theta \qquad (1)$$

where E_f is the fragment's total kinetic energy per nucleon, ε the neutron energy and θ the emission angle, both in the CM system. The angle-dependent neutron spectrum in the CM system is expressed as[1)]

$$\phi(\varepsilon,\sigma_c,\theta) = \phi(\varepsilon,\sigma_c)(1+b\cos^2\theta)/(1+b/3) \qquad (2)$$

where the anisotropy parameter b is defined as

$$b=W(\theta)/W(90^\circ) - 1. \qquad (3)$$

Then the laboratory-system spectrum of neutrons is calculated by[2)]

$$\begin{aligned} N(E,E_f,\sigma_c) &= \frac{1}{4\sqrt{E_f}}\int_{(\sqrt{E}-\sqrt{E_f})^2}^{(\sqrt{E}+\sqrt{E_f})^2}\frac{\phi(\varepsilon,\sigma_c)[1+b(E-\varepsilon-E_f)^2/4\varepsilon E_f]}{\sqrt{\varepsilon}(1+b/3)}d\varepsilon \\ &= \frac{1}{2\sqrt{E_f}T_m^2(1+b/3)}\int_{(\sqrt{E}-\sqrt{E_f})^2}^{(\sqrt{E}+\sqrt{E_f})^2}\sigma_c(\varepsilon)\sqrt{\varepsilon}d\varepsilon\int_0^{T_m}k(T)T\exp(-\varepsilon/T)dT \\ &\quad + \frac{b}{8E_f^{3/2}T_m^2(1+b/3)}\int_{(\sqrt{E}-\sqrt{E_f})^2}^{(\sqrt{E}+\sqrt{E_f})^2}\frac{\sigma_c(\varepsilon)(E-\varepsilon-E_f)^2}{\sqrt{\varepsilon}}d\varepsilon\int_0^{T_m}k(T)T\exp(-\varepsilon/T)dT \end{aligned} \qquad (4)$$

where $k(T)$ is the normalization factor given by

$$k(T) = \left[\int_0^\infty \sigma_c(\varepsilon)\varepsilon\exp(-\varepsilon/T)dT\right]^{-1}. \qquad (5)$$

3. Results

Figure 1 shows a result for $^{235}U + n_{th}$ (S2-mode) for three cases b=0, 0.1 and 0.2.

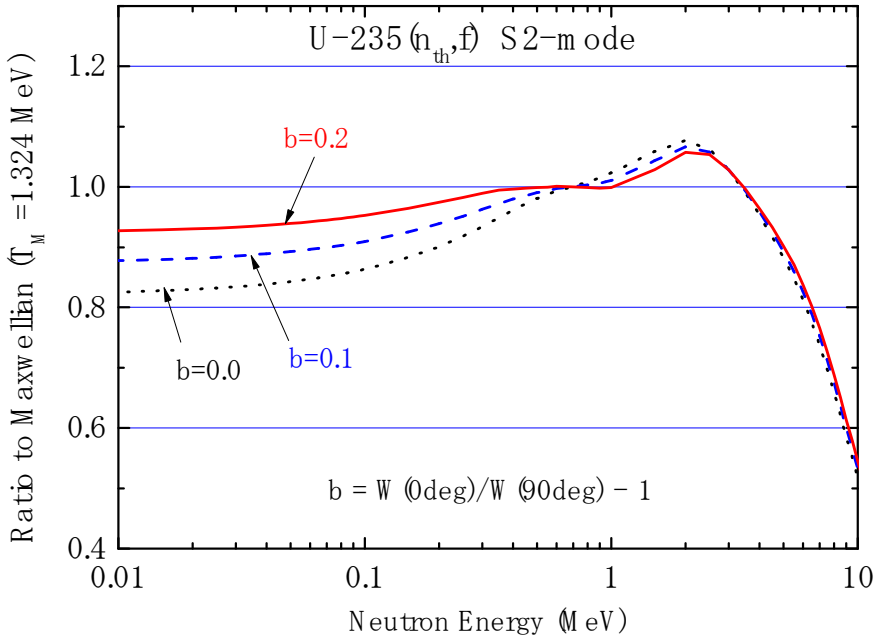

Fig.1. The effect of considering the CM-anisotropy of neutron emission.

It can be seen that consideration of angular anisotropy has the effect of enhancing the low-energy ($\leq$ 1 MeV) component of the neutron spectrum. The spectra for other fission modes show similar tendency. This result suggests that, taking into account the CM-anisotropy of neutron emission, together with accounting for NEDA (neutron emission during acceleration)-effect as described in my contribution to this meeting in the Los Alamos (Madland-Nix) model, significantly improves the agreement with experiment.

References

1) J. Terrell, Phys. Rev. **113** (1959) 527.

2) R.L. Walsh, Nucl. Sci. Eng. **102** (1989) 119.

Nuclear Data Section
International Atomic Energy Agency
P.O. Box 100
A-1400 Vienna
Austria

e-mail: services@iaeand.iaea.org
fax: (43-1) 26007
telephone: (43-1) 2600-21710
Web: http://www-nds.iaea.org